(12) INTERNATIONAL APPLICATION PUBLISHED UNDER THE PATENT COOPERATION TREATY (PCT)

(19) World Intellectual Property Organization
International Bureau

(43) International Publication Date
19 September 2019 (19.09.2019)

WIPO | PCT

(10) International Publication Number
WO 2019/175413 A1

(51) International Patent Classification:
H02K 33/02 (2006.01) *H02K 35/02* (2006.01)
H02K 7/18 (2006.01) *H02N2/18* (2006.01)

(21) International Application Number:
PCT/EP20 19/056601

(22) International Filing Date:
15 March 2019 (15.03.2019)

(25) Filing Language: English

(26) Publication Language: English

(30) Priority Data:
102018000003632 15 March 2018 (15.03.2018) IT

(71) Applicant: **UNIVERSITÀ DEGLI STUDI DELLA CAMPANIA "LUIGI VANVITELLI"** [IT/IT]; Viale A. Lincoln 5, 81100 Caserta (CE) (IT).

(72) Inventors: **VITELLI, Massimo;** Universita degli Studi della Campania "Luigi Vanvitelli" Viale A. Lincoln 5, 81100 Caserta (CE) (IT). **BALATO, Marco;** Universita degli Studi della Campania "Luigi Vanvitelli" Viale A. Lincoln 5, 81100 Caserta (CE) (IT). **COSTANZO, Luigi;** University degli Studi della Campania "Luigi Vanvitelli" Viale A. Lincoln 5, 81100 Caserta (CE) (IT). **LO SCHIAVO, Alessandro;** Universita degli Studi della Campania "Luigi Vanvitelli" Viale A. Lincoln 5, 81100 Caserta (CE) (IT).

(74) Agent: **CAPASSO, Olga** et al.; Via Vincenzo Bellini, 20, 00198 Rome (IT).

(81) Designated States *(unless otherwise indicated, for every kind of national protection available)*: AE, AG, AL, AM, AO, AT, AU, AZ, BA, BB, BG, BH, BN, BR, BW, BY, BZ, CA, CH, CL, CN, CO, CR, CU, CZ, DE, DJ, DK, DM, DO, DZ, EC, EE, EG, ES, FI, GB, GD, GE, GH, GM, GT, HN, HR, HU, ID, IL, IN, IR, IS, JO, JP, KE, KG, KH, KN, KP, KR, KW, KZ, LA, LC, LK, LR, LS, LU, LY, MA, MD, ME, MG, MK, MN, MW, MX, MY, MZ, NA, NG, NI, NO, NZ, OM, PA, PE, PG, PH, PL, PT, QA, RO, RS, RU, RW, SA, SC, SD, SE, SG, SK, SL, SM, ST, SV, SY, TH, TJ, TM, TN, TR, TT, TZ, UA, UG, US, UZ, VC, VN, ZA, ZM, ZW.

(84) Designated States *(unless otherwise indicated, for every kind of regional protection available)*: ARIPO (BW, GH, GM, KE, LR, LS, MW, MZ, NA, RW, SD, SL, ST, SZ, TZ, UG, ZM, ZW), Eurasian (AM, AZ, BY, KG, KZ, RU, TJ, TM), European (AL, AT, BE, BG, CH, CY, CZ, DE, DK, EE, ES, FI, FR, GB, GR, HR, HU, IE, IS, IT, LT, LU, LV, MC, MK, MT, NL, NO, PL, PT, RO, RS, SE, SI, SK, SM, TR), OAPI (BF, BJ, CF, CG, Cl, CM, GA, GN, GQ, GW, KM, ML, MR, NE, SN, TD, TG).

Published:
— *with international search report (Art. 21(3))*

(54) **Title:** VIBRATION ENERGY HARVESTER, OPTIMIZED BY ELECTRONICALLY EMULATED MECHANICAL TUNING TECHNIQUE

(57) Abstract: The present invention refers to a resonant vibration energy harvester **(1)** for optimizing the conversion of vibrational kinetic energy generated by an external source into electrical energy, to a system comprising such resonant vibration energy harvester and to a method for optimizing the conversion of vibrational kinetic energy generated by an external source into electrical energy.

WO 2019/175413 A1

Vibration energy harvester, optimized by electronically emulated mechanical tuning technique

TECHNICAL FIELD

The present invention relates to a resonant vibration energy harvester capable of optimizing the conversion of vibrational kinetic energy generated by an external source into electrical energy. Furthermore, the present invention relates to a system comprising said resonant vibration energy harvester. The present invention further relates to a method for optimizing the operation of said resonant harvester.

STATE OF THE ART

Resonant vibration energy harvesters (REVEHs) are devices capable of exploiting energy deriving from vibrations of the external environment that would otherwise remain unused. Energy can be extracted through transduction mechanisms that belong mainly to three broad categories: piezoelectric, electromagnetic and electrostatic transduction.

In recent years, REVEHs have been proposed for a variety of applications, such as industrial applications, medical implants, sensors inside buildings or other constructions (bridges), wireless sensor networks, etc. The use of energy harvesters eliminates all the disadvantages of using batteries to power sensors or other devices (expensive maintenance, insufficient or unpredictable operational life cycle, difficulty in replacing batteries, disposal problems, etc.).

On the other hand, however, the performance of these energy harvesters is closely linked to the vibration frequency at play. In other words, REVEHs are able to operate efficiently only when the vibration frequency of the external source corresponds to the mechanical resonance frequency of the harvester itself. This means that if the resonant vibration harvester was initially configured to oscillate at a given

resonance frequency, this should be used for those applications characterized by a dominant frequency coinciding with the resonance frequency. In practice, however, this is difficult to achieve because the environmental vibrations show a variable frequency pattern, wherein the energy content is distributed over a very wide frequency spectrum.

Various solutions have been proposed in the literature to increase the operating frequency range for resonant vibration energy harvesters. For example, arrays of resonant harvesters at different frequencies, non-linear harvesters and resonance frequency adjustment methods or tuning methods have been proposed .

Among the various tuning methods, the electric tuning method (ETT) is known which tends to adapt the electric load of the harvester by acting on the electronic parameters of the system and the mechanical tuning method (MTT) which instead tends to adjust the resonance frequency acting on the mechanical parameters of the system, such as the value of the oscillating mass and / or the stiffness of the spring.

Mechanical tuning methods can in turn be divided into passive methods, which do not require external energy and therefore are uncontrollable and not much accurate, and active methods that are more accurate but require external energy instead. In the latter case, closed-loop control schemes are used so as to guarantee automatic and roughly accurate frequency tracking.

However, although energy harvesters using active mechanical tuning systems are able to achieve good results in terms of frequency tracking, in most cases the energy consumed to achieve this goal exceeds that produced by the same harvester thus making a system of this kind not advantageous in terms of total yield as a negative final energy balance is determined.

Therefore, it is the object of the present invention to provide a resonant vibration energy harvester wherein the energy conversion is optimized by means of a new active tuning method, obtaining however a positive final energy balance.

DISCLOSURE OF INVENTION

These objects are achieved by an energy harvester, by a system and by a method according to the claims at the end of the present description.

The harvester according to the present invention is a resonant device used to optimize the conversion of vibrational kinetic energy generated by an external source into electrical energy. The harvester comprises a supporting housing capable of vibrating in response to the external source and an electromagnetic generator coupled to the housing and having a given resonance frequency. The harvester comprises elastic means placed within the housing and fixed to a wall of said housing, at least one magnetic element having a mass and coupled to the housing by said elastic means, wherein the elastic means create a relative motion among the magnetic element and the housing itself, wherein the magnetic element is a permanent magnet and the resonance frequency of the electromagnetic generator is the mechanical resonance frequency of the magnetic element with respect to the housing, and a first conductive winding, magnetically coupled to the magnetic element and fixed to the housing such that the vibrational kinetic energy generated by the external source determines a relative displacement between the magnetic element and the first winding causing a potential difference to be generated at the ends of the first winding.

The harvester is characterized in that it further comprises a second winding, or coil, fixed to a non-vibrating support and being stationary with respect to said support and separated

from the housing, wherein the distance between the first winding and the second winding is such as to make a mutual magnetic coupling between said first and second winding negligible, as well as control means connected to the ends of the second winding to inject an electric current within the second winding and regulate the intensity of said electric current so as to adapt the resonance frequency of the electromagnetic generator to the vibration frequency associated to the vibrational kinetic energy generated by the external source.

In this way, a Mechanical Tuning Technique (MTT) is determined for REVEHs based on the emulation of the desired mass-spring-damper system. Such a technique can be referred to as SMDE (Spring-Mass-Damper Emulation-based) MTT. Furthermore, the SMDE technique is an active MTT that can achieve a positive net energy balance.

The presence of a fixed external coil, added to a standard REVEH, determines a system that can be referred to as SMDE REVEH. A suitable current is circulated in such an outer coil so as to emulate, at the same time, the effects of the desired stiffness, of the desired mass and of the desired damping coefficient. Therefore, both the resonance frequency of the SMDE REVEH and its net power balance can (and must) be modified by suitably controlling the current flowing in the outer coil described above. In this way, the magnetic force that the current passing through the external coil exerts on the movable magnet of the SMDE REVEH comes to be equal to the mechanical force that would be exerted by a "virtual" spring (with the desired stiffness) on a "virtual" magnet (with the desired mass) that vibrates in a "virtual" fluid (with the desired viscous friction coefficient) .

It should be noted that the two coils (or windings) do not necessarily have to be identical in shape and size. According to alternative embodiments, it is possible to use a second coil different from the first one, however ensuring that it is fixed and that it is at a distance from the first coil such that the mutual coupling between them can be considered negligible. In the same way, it is possible to consider any configuration between the magnetic element and the two coils. Specifically, the configuration between the magnetic element and the two windings must simply comply with the condition that the second winding is fixed and that it is at such a distance from the first winding that the mutual coupling between the two windings can be considered negligible.

The proposed technique is applicable regardless of the features of the magnet and of the first winding (or internal coil) . As to the size and features of the second winding (external coil) , in the case of two identical windings, these are dictated by the first winding (internal coil) and then defined at the time of the identification of the harvester to be optimized.

According to an embodiment of the harvester, the elastic means may comprise a couple of coil springs each having one end fixed to the housing and the other end fixed to the magnetic element. In this way, the magnetic element is movable and free to vibrate inside the housing. The elastic means can be any type of means able to guarantee the relative movement between the magnetic element and the housing in response to the vibration of the generator. Depending on the particular configuration of the housing and / or the magnet, the elastic means may vary in number .

According to a further embodiment, in order to extract the electric current produced as a result of the vibration of the external source, the harvester can further comprise an

extraction electrical circuit and a storage circuit coupled to the ends of the first winding.

In one embodiment of the harvester according to the present description, the first and second windings can be positioned at opposite sides with respect to the magnetic element. In this way, the electromagnetic coupling between the two coils or windings can be reduced.

In particular, the control means may comprise a control electrical circuit for the generation of electrical current and the consequent emulation of a mass-spring-damper system.

Furthermore, the control electrical circuit is configured to determine an emulated resonance frequency with a value that is higher than the vibration frequency (of the external source) and lower than the mechanical resonance frequency of the electromagnetic generator.

The system according to the present invention comprises a resonant vibration energy harvester according to one of the preceding claims and an electronic device coupled to said harvester .

The method for optimizing the conversion of vibrational kinetic energy generated by an external source into electrical energy according to the present invention comprises the step of providing a supporting housing capable of vibrating in response to the external source and of coupling to the housing an electromagnetic generator having a resonance frequency, wherein the harvester comprises elastic means placed within the housing and fixed to a wall of said housing, at least one magnetic element having a mass and coupled to the housing by said elastic means, wherein the elastic means create a relative motion among the magnetic element and the housing itself and wherein the magnetic element is a permanent magnet and the resonance frequency of the electromagnetic generator is the

mechanical resonance frequency of the magnetic element with respect to the housing and a first conductive winding, magnetically coupled to the magnetic element and fixed to the housing such that the vibrational kinetic energy generated by the external source determines a relative displacement between the magnetic element and the first winding causing a potential difference to be generated at the ends of the first winding.

The method is characterized by providing a second winding, fixed to a non-vibrating support and being stationary with respect to said support and separated from the housing, wherein the distance between the first winding and the second winding is such as to make a mutual magnetic coupling between said first and second winding negligible, as well as connecting control means to the ends of the second winding to inject an electric current within the second winding and regulate the intensity of said electric current so as to adapt the resonance frequency of the electromagnetic generator to the frequency or frequencies associated to the vibrational kinetic energy generated by the external source.

This method is used to optimize the conversion of vibrational energy into electrical energy on the basis of an energy harvester as previously described. Therefore, all the advantages and features of the harvester also apply to the associated optimization method.

According to an embodiment, the step of connecting the control means to the ends of the second winding determines the emulation of a mass-spring-damper system.

These and other aspects of the present invention will become more apparent by reading the following description of some preferred embodiments described below.

Fig. 1 shows a schematic representation of a conventional REVEH;

Figs. 2a-b show a single degree of freedom model of a conventional REVEH (a), a corresponding equivalent circuit (b) and the qualitative pattern of power as a function of frequency (c);

Fig. 3 is a schematic representation of an energy harvester according to an embodiment of the present invention;

Figs. 4a-b show the forces acting on the movable magnet of the harvester according to an embodiment of the present invention (a) and the corresponding equivalent electrical circuit (b);

Fig. 5 shows the architecture of an SMDE MTT REVEH system according to an embodiment of the present invention;

Fig. 6 shows in a graph the value of $\Delta P\%$ as a function of m^*/m and ksVks; $c^*/c = -1.6$ and $f_{vib}/f_{opt} = 0.8$;

Figs. 7a-d show in a graph the value of $\Delta P_{MAX}\%$ as a function of c^*/c at $f_{vib}/f_{0pt} = 0.8$ (a), the value of $m_{BE}s_T^*/m$ as a function of c^*/c at $f_{vib}/f_{0pt} = 0.8$ (b), the value of $ks_{BE}s_T^*/ks$ as a function of c^*/c at $f_{vib}/f_{opt} = 0.8$ (c) and the value of $f^*_{opt\_BEST}/f_{vib}$ as a function of c^*/c;

Fig. 8 shows the pattern of $\Delta P\%$ as a function of m^*/m and ksVks; cVc = c_{BEST} v c = -0.4 and $f_{vib}/f_{opt} = 0.8$;

Figs. 9a-c show the pattern, as a function of frequency, of the main powers taken into consideration, $c^*/c = c_{BEST}$ = -0.4 and $f_{vib}/f_{opt} = 0.8$ (a), the load voltages V_{LOAD_SMDE} and V, the output voltage of the electronic power converter V_{ext}, $c^*/c = c_{BEST}$ = -0.4 and $f_{vib}/f_{opt} = 0.8$ (b) and the load currents I_{SMDE} and I, current in the external coil I_{ext}, $c^*/c = -0.4$ and $f_{vib}/f_{opt} = 0.8$ (c);

Fig. 10 shows the pattern of $\Delta P\%$ as a function of m^*/m and ksVks; cVc = c_{BEST} v c = -0.2 and $f_{vib}/f_{opt} = 0.7$;

Figs, lla-c show the pattern as a function of frequency of the main powers taken into consideration, $c^*/c = c_{BEST}$ v c = -0.2 and f_{vib}/f_{0pt} = 0.7 (a), the load voltages V_{LOAD_SMDE} and V, the output voltage of the electronic power converter V_{ext}, c^*/c = c_{BEST} v c = -0.2 and f_{Vib}/f_{opt} = 0.7 (b) and the load currents I_{SMDE} and I, current in the external coil I_{ext}, $c^*/c = c_{BEST}{}^*/c$ = -0.2 and f_{vib}/f_{0pt} = 0.7 (c) .

As highlighted earlier, the SMDE technique is an active MTT. This means that, obviously, it will only be useful from the practical point of view in those operating conditions wherein the power required for the implementation of the technique itself (P_{SMDE}) is less than the power that SMDE REVEH provides at its optimal load (P_{LOAD_SMDE}). It should be noted that the requirement that the extracted net power P_{LOAD_SMDE} - P_{SMDE} is positive is not sufficient. In particular, due to the fact that a second coil is added to the starting REVEH, the performance of the resulting harvester (SMDE REVEH) cannot be compared only with those of the ORIGINAL REVEH, i.e. the conventional harvester without an external coil. In the following, the REVEH obtained by connecting in series the original coil with the external coil will be called SERIES REVEH and the power it provides to its optimal load will be referred to as P_{SERIES}. The REVEH obtained by replacing the original coil with the external coil will be called EXTERNAL REVEH and the power it provides to its optimal load will be referred to as $P_{EXTERNAL}$. For a correct performance analysis, the reference power $P_{BENCHMARK}$ must coincide with the maximum between the powers P_{SERIES}, $P_{EXTERNAL}$ and $P_{0RIGINAL}$ (power that the ORIGINAL REVEH supplies to its optimal load) . This means that the SMDE technique will be useful from a practical point of view only if the extracted net power (P_{LOAD_SMDE} - P_{SMDE}) is greater than the reference power $P_{BENCHMARK}$. The present invention shows how

to maximize the quantity $P_{LOAD-SMDE} - P_{SMDE} - P_{BENCHMARK}$ at a desired vibration frequency f_{vib}.

Figure 1 schematically shows the structure of a conventional REVEH energy harvester 11. A permanent magnet 13 having a mass m is connected to a system of springs 12 (the springs 12 are positioned on the sides of the magnet 13) and moves, in the presence of the vibrations, into the housing 10 of the REVEH. A coil 14 (or internal coil in Fig. 1) is fixed to the housing 10 and a load 18 is present on its ends. Following the vibrations, a relative displacement x(t) is created between the magnet 13 and the coil 14. This relative displacement x(t) allows the conversion of mechanical energy into electrical energy. y(t) represents the displacement of the base of the housing 10 with respect to a fixed reference.

The device in figure 1 can be represented by a Single Degree of Freedom (SDOF) model shown in Figure 2(a) where the forces acting on the magnet are represented by means of appropriate arrows. In particular, $c\text{-}x(t)$ represents the viscous friction force (wherein c is the viscous friction coefficient), $k_s\text{-}x(t)$ represents the elastic force exerted by the spring system (wherein k_s is the equivalent elastic constant of the spring system in Fig. 1), $\theta_{int} \cdot i(t)$ represents the electromagnetic force due to the coil (wherein $d_{\pm nt}$ is the electromechanical coupling coefficient of the coil inside the harvester) .

The application of the second law of Newton, along the axis z, to the SDOF system of Fig. 2 leads to the writing of the following equation which regulates the behaviour in time of the relative displacement x(t) :

$$\frac{m}{\theta_{int}}\ddot{x}(t)+\frac{c}{\theta_{int}}\dot{x}(t)+\frac{k_s}{\theta_{int}}x(t)+i(t)=-\frac{m}{\theta_{int}}\ddot{y}(t)$$

Equation (1)

wherein *m* represents the value of the oscillating mass (mass of the magnet 13) and $\ddot{y}(t)$ represents the acceleration to which the housing 10 of the REVEH is subjected. Since each addend of equation (1) is an electrical current, it is possible to identify the equivalent electrical circuit of the REVEH as shown in figure 2(b).

In particular, in figure 2(b), L_{c_int} and R_{c_int} respectively represent the inductance and resistance of the internal coil 14, $i(t)$ represents the current flowing into the load 18 and $\varepsilon(t)$ is the electromotive force (emf) induced in the inner coil 14. The expression of this emf is as follows:

$$\varepsilon(t) = \dot{\chi}(t)\theta_{in1}$$

Equation (2)

If we consider a sinusoidal type acceleration of the housing 10 $\ddot{y}(t)$ with a pulsation ω (i.e. $\ddot{y}(t) = a\cdot\cos(\omega t)$), equations (1) and (2) can be rewritten in the domain of frequency and become equations (3) and (4), respectively:

$$\frac{m}{\Theta_{int}}\left[-\omega^2 X(\omega)\right] + \frac{j\omega X(\omega)}{\Theta_{int}} + \frac{1}{\Theta_{int}} X(\omega) + I(\omega) = -\frac{a}{\Theta_{int}}$$

Equation (3)

$$E(\omega) = j\omega X(\omega)\cdot\theta_{int}$$

Equation (4)

wherein $X(\omega)$, $I(\omega)$ and $E(\omega)$ respectively represent the Fourier transform of $x(t)$, $i(t)$ and $\varepsilon(t)$ and j is the imaginary unit. By analysing the circuit of figure 2(b) it is possible to obtain :

$$E(\omega) = I(\omega)\cdot\left[R_{c\_int} + R_L + j\cdot\left(X_{c\_int}(\omega) + X_L(\omega)\right)\right]$$

Equation (5)

where :

$$X_{c\_int}(\omega) = \omega\cdot L_{c\_int}$$

$$X_L(\omega) = \omega\cdot L_L - \frac{1}{\omega\cdot C_L}$$

Equation (6)

From equations (4) and (5) it is possible to write the following expression of the relative displacement $X(\omega)$:

$$X(\omega) = I(\omega) \cdot \frac{\left[R_{c\_int} + R_L + j \cdot \left(X_{c\_int}(\omega) + X_L(\omega)\right)\right]}{j M \theta_{int}}$$

Equation (7)

Therefore, inserting the equation (7) in (3), we obtain:

$$I(\omega) = \frac{-m \cdot a \cdot j\omega\theta_{int}}{\left[R_{c\_int} + R_L + j \cdot \left(X_{c\_int}(\omega) + X_L(\omega)\right)\right] \cdot \left(k_s - m \cdot \omega^2 + j\omega c\right) + j\omega\theta_{int}^2}$$

Equation (8)

Finally, the power transferred to the load is equal to:

$$P_{load}\left(R_L, X_L, \omega\right) = \frac{1}{2} R_L \left|I(\omega)\right|^2$$

Equation (9)

The optimal load, i.e. the load that maximizes $P_{load}(\omega)$ at a certain frequency is:

$$X_{L\_opt}(\omega) = \frac{\theta_{int}^2 \left(m \cdot \omega^2 - k_s\right)\omega}{\left(k_s - m \cdot \omega^2\right)^2 + \left(c\omega\right)^2} - X_{c\_int}(\omega)$$

Equation (10.1)

$$R_{L\_opt}(\omega) = R_{c\_int} + \frac{\theta_{int}^2 c \cdot \omega^2}{\left(k_s - m \cdot \omega^2\right)^2 + \left(c\omega\right)^2}$$

Equation (10.2)

As a consequence, the expression of the maximum power $P_{ORIGINAL}(\omega)$ supplied by the conventional REVEH to the load is as follows:

$$P_{ORIGINAL}(\omega) = P_{load}\left(R_{L\_opt}(\omega), X_{L\_opt}(\omega), \omega\right) = \frac{1}{8} \frac{a^2 \theta_{int}^2 m^2 \omega^2}{R_{c\_int}\left[\left(k_s - m\omega^2\right)^2 + (cco)^2\right] + c(co0_{int})^2}$$

Equation (11)

Figure 2c shows the typical $P_{ORIGINAL}$ pattern as a function of frequency. Due to the resonant nature of the REVEH, maximum

power is supplied to the optimal load only at the resonance frequency f_{opt} of the mass-spring-damper system. The values of such resonance frequency ($f_{opt} = \omega_{opt}/(2n)$) and of the maximum extractable power $P_{QRIGINAL-MAX} = P_{ORIGINAL}(\omega_{opt})$ are as follows:

$$\omega_{opt} = 2 \cdot \pi \cdot f_{opt} = \sqrt{\frac{k_s}{m}}$$

Equation (12)

$$P_{ORIGINAL\_MAX} = P_{ORIGINAL}\left(\omega_{opt}\right) = \frac{1}{8} \frac{a^2 \theta_{int}^2 m^2}{R_{c\_int} \cdot c^2 + c \cdot \theta_{int}^2}$$

Equation (13)

In practice, if the vibration frequency f_{vib} varies with time, any ETT technique ideally allows to extract only the power that is given by the curve shown in Fig. 2c at the vibration frequency f_{Vib} - On the contrary, since the SMDE technique is an MTT, when it is coupled to any ETT technique, it ideally allows (i.e. when P_{SMDE} is null) to extract the power peak $P_{ORIGINAL\_MAX}$ at each frequency. In other words, it allows to extract the power peak of the time-varying curve which is obtained by moving the curve of Fig. 2c, right or left, as desired. In practice, however, due to the presence of a non-zero $P_{SMDE}(\omega)$, the net power extracted $P_{LOAD\_SMDE}(2nf_{Vib}) - P_{SMDE}(2nf_{Vib})$ at the frequency f_{vib}, is less than $P_{0RIGINAL\_MAX}$. However, this net power is greater than $P_{0RIGINAL}(2nf_{vib})$. As shown below, due to the particular trends of $P_{LOAD-SMDE}(\omega)$, $P_{SMDE}(\omega)$ and $P_{BENCHMARK}(\omega)$, in order to obtain the maximum value of $P_{LOAD\_SMDE}(2nf_{Vib}) - P_{SMDE}(2nf_{vib}) - P_{BENCHMARK}(2nf_{vib})$ it is necessary to regulate appropriately the values of the equivalent stiffness, of the equivalent mass and of the equivalent viscous friction coefficient. Through this adjustment, an optimal mechanical resonance frequency f_{opt}^* (greater than f_{vib}) of the SMDE REVEH is obtained. In other words, if the vibration frequency f_{vib} varies over time, the joint use of SMDE MTT and of any ETT is

necessary in order to fully optimize the performance of a REVEH harvester .

According to the present invention, a SMDE MTT technique is proposed. This technique is based on the use of an external coil 15 through which an appropriate current passes with the aim of emulating adjustable stiffness, mass and viscous friction coefficient values. In particular, the adjustable stiffness will be expressed as $k_s + k_s^*$, the adjustable mass as $m + m^*$ and the adjustable viscous friction coefficient as $c + c^*$. It should be noted that k_s^*, m^* and c^* can be greater than or less than zero as they represent suitable variations with respect to the corresponding original quantities (k_s, m and c). The desired current which must flow into the external coil 15 can be regulated by the use of an appropriate power electronics circuit or electrical control circuit 17. It should be noted that the control of the harvester according to the present invention, i.e. the SMDE REVEH (and its architecture) is certainly easier to implement than the mechanical actuators belonging to the state of the art. The parameters of the external coil 15 are as follows: resistance R_{c_ext}, inductance L_{c_ext} and electromechanical coupling coefficient $@_{ext}$. A schematic representation of the harvester according to the present invention (SMDE REVEH) is shown in figure 3. In addition to the elements present in a conventional harvester shown in figure 1, the harvester SMDE REVEH comprises a coil 15 outside the housing 10.

The substantial difference between the inner coil 14 and the outer coil 15 is represented by the fact that the first is connected to the housing 10 of the REVEH and moves integral with it, while the second is anchored to a fixed point. In practice, this has repercussions on the emf induced in the two coils. In particular, the emf induced in the internal coil 14

will be equal to $\Theta i_{nt} \cdot \dot{x}_{SMDE}(t)$ (the SMDE subscript is used to indicate the fact that the SMDE MTT technique is applied), while that induced in the external coil 15 will be given by $\Theta_{ext} \cdot [\dot{x}_{SMDE}(t)+\dot{y}(t)]$. It should be noted that in the following the mutual electromagnetic coupling between the two coils will be considered negligible. This simplifying hypothesis is reasonable because the two coils are placed at opposite sides of the magnet 13 which vibrates and therefore at a relatively large distance from each other (see Fig. 3). In fact, as is well known, to maximize the electromechanical coupling coefficient Θ between each coil 14, 15 and the magnet 13, the distance between each of these and the magnet itself cannot be less than a certain optimal distance.

The injection of current into the external coil 15 is intended to emulate, through the electromagnetic force $\Theta_{ext'iext}(t)$ exerted on the magnet 13, the sum of three additional forces as shown in Fig. 4a. These forces are $k_S^* \cdot x_{SMDE}(t)$ (elastic force), $m^* \cdot [\ddot{x}_{SMDE}(t)+\ddot{y}(t)]$ (inertial force) and $c^* \cdot \dot{x}_{SMDE}(t)$ (viscous friction force).

The application along the axis z of Newton's second law to the system of Fig. 4a leads to the writing of the following equation which regulates the pattern in time of the relative displacement $x_{SMDE}(t)$ between the magnet 13 and the internal coil 14:

$$\frac{m+m^*}{\theta_{int}}\ddot{x}_{SMDE}(t)+\frac{c+c^*}{\theta_{int}}\dot{x}_{SMDE}(t)+\frac{k_s+k_s^*}{\theta_{int}}x_{SMDE}(t)+i_{SMDE}(t)=-\frac{m+m^*}{\theta_{int}}\ddot{y}(t)$$

Equation (14)

In the equation (14) the SMDE subscript was used to underline the fact that the SMDE MTT technique is applied. In practice, equation (14) was obtained from equation (1) substituting k_s with $k_s + k_s^*$, m with $m + m^*$ and c with $c + c^*$. The emf which is induced in the inner coil 14 is therefore:

$$\varepsilon_{SMDE}(t)=\dot{x}_{SMDE}(t)\theta_{int}$$

Equation (15)

So the new resonance frequency f_{opt}^{*} will be:

$$\omega_{opt}^{*}=2\pi f_{opt}^{*}=\sqrt{\frac{k_s+k_s^{*}}{m+m^{*}}}$$

Equation (16)

In conclusion, the objective of the SMDE MTT technique is to apply a Lorentz force $0_{ext'iext}(t)$ to the magnet 13 in order to emulate the three desired additional forces (Fig. 4a). This result can be achieved by regulating the current $i_{ext}(t)$ in the external coil 15 so that the electromagnetic force exerted by it on the magnet $0_{ext'iext}(t)$ is exactly equal to the desired force (equation (17)):

$$Fext=-\theta_{ext}\cdot i_{ext}(t)=-k_s^{*}\cdot x_{SMDE}(t)-c^{*}\cdot\dot{x}_{SMDE}(t)-m^{*}\cdot(\ddot{x}_{SMDE}(t)+\ddot{y}(t))$$

Equation (17)

The electrical circuit equivalent to the equation (14) is shown in Fig. 4b. Note that the circuit in Fig. 4b coincides with the circuit of Fig. 2b provided that the inductance θ_{int}^{2}/k_s is replaced with the inductance $\theta_{i\eta i}^{2}/(k_s+k_s^{*})$, the capacity m/di_{nt}^{2} is replaced with the capacity $(m+m^{*})/\theta_{int}^{2}$ and the resistance $\theta_{i\eta i}^{2}/C$ is replaced with the resistance $\theta_{i\eta i}^{2}/(c+c^{*})$. In the case where $k_s^{*}=0$, $m^{*}=0$ and $c^{*}=0$, $x_{SMDE}(t)=x(t)$ is obtained; otherwise, $x_{SMDE}(t)\neq x(t)$.

The current in the load in Fig. 4b takes the following expression :

$$I_{SMDE}(\omega)=\frac{-(m+m^{*})\cdot a\cdot j\omega\theta_{int}}{\left[\left[R_{c\_int}+R_L+j\cdot\left(X_{c\_int}(\omega)+X_L(\omega)\right)\right]\cdot\left[\left(k_s+k_s^{*}\right)-(m+m^{*})\cdot\omega^{2}+jco(c+c^{*})\right]+j\omega\theta_{in_t}{}^{2}\right]}$$

Equation (18)

In practice, equation (18) was obtained from equation (8) replacing k_s with $k_s+k_s^{*}$, m with $m+m^{*}$ and c with $c+c^{*}$. The

load impedance that maximizes the power supplied to the load at a given frequency assumes the following expression:

$$X_{L\_opt\_SMDE}(\omega)=\frac{\theta_{int}^{2}\left[(m+m^{*})\cdot\omega^{2}-\left(k_{s}+k_{s}^{*}\right)\right]\omega}{\left[\left(k_{s}+k_{s}^{*}\right)-(m+m^{*})\cdot\omega^{2}\right]^{2}+\left((c+c^{*})\omega\right)^{2}}-X_{c\_int}$$

Equation (19.1)

$$R_{L\_opt\_SMDE}(\omega)=R_{c\_int}+\frac{\theta_{int}^{2}(c+c^{*})\cdot\omega^{2}}{\left[\left(k_{s}+k_{s}^{*}\right)-(m+m^{*})\cdot\omega^{2}\right]^{2}+\left((c+c^{*})\omega\right)^{2}}$$

Equation (19.2)

In practice, equations (19.1 and 19.2) were obtained from equations (10.1 and 10.2) by replacing k_s with $k_s + k_s^*$, m with $m + m^*$ and c with $c + c^*$. The power $P_{LOAD\_SMDE}(R_{L-opt-SMDE}(\omega), X_{L-opt-SMDE}(\omega), \omega)$ supplied to this optimal load is equal to:

$$P_{LOAD\_SMDE}\left(R_{L\_opt\_SMDE}(\omega),X_{L\_opt\_SMDE}(\omega),\omega\right)=$$

$$=\frac{1}{8}\frac{a^{2}\theta_{int}^{2}(m+m^{*})^{2}\omega^{2}}{R_{c\_int}\left[\left(k_{s}+k_{s}^{*}-(m+m^{*})\omega^{2}\right)^{2}+\left((C+C^{*})\omega\right)^{2}\right]+(c+c^{*})(\omega\theta_{int})^{2}}$$

Equation (20)

In practice, also equation (20) was obtained from equation (11) replacing k_s with $k_s + k_s^*$, m with $m + m^*$ and c with $c + c^*$. Note that, at the new resonance frequency f_{opt}^*, we have:

$$P_{LOAD\_SMDE\_MAX}=\frac{1}{8}\frac{a^{2}\theta_{int}^{2}(m+m^{*})^{2}}{R_{c\_int}(c+c^{*})^{2}+(c+c^{*})\theta_{int}^{2}}$$

Equation (21)

By using equation (17) it is possible to obtain the expression of the current which must be injected into the external coil 15 in order to obtain the emulation of the desired additional force :

$$i_{ext}(t)=\frac{k_{s}^{*}\,x_{SMDE}(t)+c^{*}\,\dot{x}_{SMDE}(t)+m^{*}\,\ddot{x}_{SMDE}(t)}{\theta_{ext}}$$

Equation (22)

Obviously, in order to implement the SMDE MTT technique, a certain non-zero power P_{SMDE} is required. It is therefore necessary to evaluate this power. In particular, using the <β> symbol to identify the average of the time-varying quantity $\beta(t)$ (over a time interval of $2\pi/\omega$), it must be:

$$P_{SMDE} = \langle i_{ext}(t) \cdot v_{ext}(t) \rangle = \left\langle i_{ext}(t) \cdot \left[R_{c\_ext} \cdot i_{ext}(t) + L_{c\_ext} \cdot \frac{di_{ext}(t)}{dt} - \theta_{ext} \cdot (\dot{x}_{SMDE}(t) + \dot{y}(t)) \right] \right\rangle =$$

$$= \frac{1}{2} R_{c\_ext} \left| I_{ext}(\omega) \right|^2 - \langle \theta_{ext} \cdot (\dot{x}_{SMDE}(t) + \dot{y}(t)) \cdot i_{ext}(t) \rangle$$

Equation (23)

where $v_{ext}(t)$ represents the voltage at the output of the power electronics converter which regulates the current in the external coil 15 (see Fig. 5). We have:

$$\langle \theta_{ext} \cdot (\dot{x}_{SMDE}(t) + \dot{y}(t)) \cdot i_{ext}(t) \rangle =$$

$$= \left\langle \theta_{ext} \cdot (\dot{x}_{SMDE}(t) + \dot{y}(t)) \cdot \frac{k_s^* \cdot x_{SMDE}(t) + c^* \cdot \dot{x}_{SMDE}(t) + m^* \cdot (\ddot{x}_{SMDE}(t) + \ddot{y}(t))}{\theta_{ext}} \right\rangle =$$

$$= \langle k_s^* \cdot x_{SMDE}(t)\, \dot{y}(t) + c^* \cdot (\dot{x}_{SMDE}(t))^2 + c^* \cdot \dot{x}_{SMDE}(t)\, \dot{y}(t) \rangle$$

Equation (24)

Then :

$$P_{SMDE} = \frac{1}{2} R_{c\_ext} \left| I_{ext}(\omega) \right|^2 - \frac{1}{2} k_s^* \cdot \mathrm{Re}\left\{ X_{SMDE}(\omega) \cdot j\frac{a}{\omega} \right\} - \frac{1}{2} c^* \cdot \left| \omega X_{SMDE}(\omega) \right|^2 - \frac{1}{2} c^* \cdot \mathrm{Re}\{ -X_{SMDE}(\omega) \cdot$$

Equation (25)

Since P_{SMDE} depends on $I_{ext}(\omega)$ and $X_{SMDE}(\omega)$, it is necessary to evaluate the final expression of such quantities. The equations (14) and (15) written in the frequency domain become:

$$\frac{m+m^*}{\theta_{int}} \left[-\omega^2 X_{SMDE}(\omega) \right] + \frac{c+c^*}{\theta_{int}} \left[j\omega X_{SMDE}(\omega) \right] + \frac{k_s + k_s^*}{\theta_{int}} X_{SMDE}(\omega) + I_{SMDE}(\omega) = -\frac{m+m^*}{\theta_{int}} a$$

Equation (26)

$$E_{SMDE}(\omega) = j\omega X_{SMDE}(\omega) \cdot \theta_{int}$$

Equation (27)

Furthermore, the loop equation represented by the internal coil 14 is:

$$I_{SMDE}(\omega)\cdot\left[R_{c\_int}+R_L(\omega)+j\cdot\left(X_{c\_int}(\omega)+X_L(\omega)\right)\right]=E_{SMDE}(\omega)=j\omega X_{SMDE}(\omega)\cdot\theta_{int}$$

Equation (28)

Then the following relation is obtained:

$$I_{SMDE}(\omega)=X_{SMDE}(\omega)\cdot\frac{j\omega\theta_{int}}{\left[R_{c\_int}+R_L(\omega)+j\cdot\left(X_{c\_int}(\omega)+X_L(\omega)\right)\right]}$$

Equation (29)

Using equations (26) and (29), the following expression of $X_{SMDE}(\omega)$ is obtained:

$$X_{SMDEC®)}=-\frac{(m+m^*)\cdot a}{\left[-\omega^2\cdot(m+m^*)+j\omega\cdot(c+c^*)+k_s+k_s^*+\frac{j\omega\theta_{int}^2}{\left[R_{c\_int}+R_L(\omega)+j\cdot\left(X_{c\_int}(\omega)+X_L(\omega)\right)\right]}\right]}$$

Equation (30)

At this point $I_{ext}(\omega)$ can be evaluated by rewriting the equation (22) in the frequency domain:

$$I_{ext}(\omega)=\frac{k_s^*\cdot X_{SMDE}(\omega)+c^*\cdot j\omega X_{SMDE}(\omega)+m^*\cdot(-\omega^2 X_{SMDE}(\omega)+a)}{\theta_{ext}}$$

Equation (31)

Equations (30) and (31) provide the desired expressions of $I_{ext}(\omega)$ and $X_{SMDE}(\omega)$ that are necessary to evaluate the power P_{SMDE} (see equation (25)).

As discussed above, the practical utility of the proposed SMDE MTT technique is closely linked to the values assumed by $P_{LOAD\text{-}SMDE}(2nf_{vib})$ - $P_{SMDE}(2nf_{vib})$ (net mean power extracted by applying SMDE MTT) and by $P_{BENCHMARK}(2nf_{Vib})$. $P_{BENCHMARK}(2nf_{vib})$ represents the maximum among $P_{SERIES}(2nf_{vib})$, $P_{ORIGINAL}(2nf_{vib})$ and $P_{EXTERNAL}(2nf_{vib})$. In the following, for simplicity but without any loss of generality, an external coil 15 identical to the internal coil 14 *(Rc_ext = Rc_int r Rc_ext = L_{c_int}* and *Qext = Qint)* will be considered. If the external coil 15 is identical to

the internal coil 14 then $P_{ORIGINAL}(2nf_{Vib}) = P_{EXTERNAL}(2nf_{vib})$ and therefore $P_{BENCHMARK}(2nf_{vib})$ will be the maximum between $P_{SERIES}(2nf_{vib})$ and $P_{ORIGINAL}(2nf_{vib})$ only. In practice, the need to consider $P_{SERIES}(2nf_{vib})$, in addition to $P_{ORIGINAL}(2nf_{vib})$, is linked to the fact that, since the use of an additional coil is intended for the implementation of the SMDE MTT technique, it is also fair to consider the possible improvement of performance that can be obtained by using also this external coil 15 in the standard way. Note that, in the case of the SERIES REVEH, both the external and the internal coil, which are connected in series, are anchored to the housing of the harvester. This means that there is no relative displacement between the two coils as it happens in the case of SMDE REVEH. Obviously, the series connection of the coils in the SERIES REVEH involves the increase of the electromechanical coupling coefficient (desired effect) but also the increase of resistance (undesired effect) . On the basis of the previous discussion, the expression of $P_{SERIES}(\omega)$ can be easily obtained considering that the electromechanical coupling coefficient of SERIES REVEH is equal to $\theta_{int} + \theta_{ext}$, the total inductance of its coil is equal to $L_{c\_int} + L_{c\_ext}$ and the total resistance of its coil is $R_{c\_int} + R_{c\_ext}$.

Then :

$$P_{SERIES}(\omega) = \frac{1}{8} \frac{a^2 (\theta_{int} + \theta_{ext})^2 m^2 \omega^2}{\left(R_{c\_int} + R_{c\_ext}\right)\left[(k_s - m\omega^2)^2 + (c\omega)^2\right] + c(\omega\theta_{\omega t} + \omega\theta_{ext})^2}$$

Equation (32)

Obviously, for the SERIES REVEH to extract the power $P_{SERIES}(\omega)$, it is necessary to use the following optimal load $R_{L\_opt\_series}(\omega) + j\, X_{L\_opt\_series}(\omega)$:

$$\mathbf{X}_{L\_opt\_series}(\omega)=\frac{(\theta i_{„t}+\theta_{ext})^2\,(m\cdot\omega^2-k_s)\,\omega}{\left(k_s\text{-}m\text{-}co^{\,2}\right)^2+(cco)^2}\text{"}\left(X_{c\_int\,(®)}+X_{c\_cxt\,(“)}\right)$$

Equation (33.1)

$$\mathbf{R}_{L\_opt\_series}(\omega)=R_{c\_int}+R_{c\_ext}+-\frac{(\theta_{int}+\theta_{ext})^2\,c\text{-}\omega^2}{\left(k_s\text{-}m\text{-}co^2\right)^2+(cco)^2}-$$

Equation (33.2)

In conclusion, the SMDE MTT technique is only useful if:

$$P_{LOAD\_SMDE}(2\pi f_{vib})-P_{SMDE}(2\pi f_{vib})>P_{BENCHMARK}(^2\pi fvib)$$

Equation (34)

Furthermore, in order to maximize the quantity $P_{LOAD\_SMDE}(2nf_{vib})$ - $P_{SMDE}(2nf_{vib})$ - $P_{BENCHMARK}(2nf_{vib})$, in general it must be f_{opt}^{*} + f_{vib} - In other words, as shown below, in order to obtain the optimal performance of the SMDE MTT technique at the frequency f_{vib}, it is necessary to set the new mechanical resonance frequency f_{opt}^{*} to a different value with respect to the vibration frequency f_{Vib} -

Fig. 5 shows the architecture of the entire SMDE MTT REVEH 20 system. Applications of this type of system include, for example, the supply of sensors for environmental monitoring, the powering of monitoring and industrial control and safety systems, the feeding of wireless sensor networks and the power supply of electronic devices for the Internet of Things. Moreover, the greater availability of energy, which the proposed system guarantees compared to existing systems, makes it possible to extend the practical uses of existing vibration harvesters to user systems that require higher levels of energy .

It is worth noting that the components of the architecture shown in Figure 5 enclosed within the dotted box at the bottom constitute the control circuit 25 of the current to be injected

into the second coil or external coil 15 so as to obtain the emulation of the mass-spring-damper system.

The system includes the ORIGINAL REVEH energy harvester as previously described, the equivalent circuit of which is indicated by the reference 24 in figure 5 and an external coil. A battery 21 is powered by an internal active AC/DC converter 22 (the AC/DC converter connected to the internal coil 14, AC/DC Converter 1). The direction of the energy flow through this converter 22 is from the internal coil 14 to the battery / load ($PLOAD\_SMDE > 0$). Moreover, this battery 21 is also connected to the external coil 15 by means of a second electronic power converter 23 (AC/DC Converter 2). As shown successively, the direction of the energy flow through this converter 23 may be from the battery 21 towards the external coil 15 ($P_{SMDE} > 0$) or from the external coil 15 towards the battery / load ($PSMDE < 0$). Obviously, in order to implement the SMDE MTT technique, as shown in Fig. 5, it is necessary to know $x_{SMDE}(t)$, $\dot{x}_{SMDE}(t)$, $\ddot{x}_{SMDE}(t)$ and y(t) (see equation (22)). In practice, in order to obtain such quantities, it is sufficient to know $\dot{x}_{SMDE}(t)$ and $\dot{x}_{SMDE}(t) + y(t)$. $\dot{x}_{SMDE}(t)$ can be obtained by measuring the open circuit voltage ($\Theta_{measure\_1} \cdot \dot{x}_{SMDE}(t)$) of a sensing coil 1 operating in an open circuit and anchored to the SMDE REVEH housing 10 (like the internal coil 14). $0_{measure\_1}$ is the electromechanical coupling coefficient of this sensing coil 1. Instead, $\dot{x}_{SMDE}(t) + y(t)$ can be obtained by measuring the open circuit voltage ($0_{measure\_2} \cdot [x_{SMDE}(t) + y(t)]$) of a sensing coil 2 operating in open circuit and anchored to a fixed point (like the outer coil 15). $0_{measure\_2}$ is the electromechanical coupling coefficient of this sensing coil 2. What will be analysed in detail later is the energy balance of the system of Fig. 5. The results that are shown and discussed have been obtained assuming an ideal functioning of both the

internal active AC/DC converter and the one connected to the external coil 15. In other words, it will be assumed that the currents that circulate both in the external coil 15 and in the internal coil 14 are perfectly sinusoidal.

With the help of the results of a series of numerical simulations it is possible to demonstrate the validity of the SMDE MTT technique. In particular, two REVEH harvesters are considered. The first considered REVEH (REVEH 1) has the following mechanical parameters: m = 0.022 kg, k_s = 3371 N/m, c = 0.345 N-s/m, θ_{int} = 5.64 N/A, $R_{c\text{-}int}$ = 1.6 Ω, $L_{c\text{-}int}$ = 250 µH. Its resonance frequency is f_{opt} = 62.3 Hz. At a = 1 g (peak acceleration value) and at the resonance frequency, REVEH 1 is able to supply to its optimal load a power equal to P_{MAX} = 16.5 mW. In the following, the ΔP% symbol will indicate the quantity defined as follows:

$$\Delta P\% = \frac{P_{LOAD\ \ SMDE}(f_{vib}) - P_{SMDE}(f_{vib}) - P_{BENCHMARK}(f_{vib})}{P_{BENCHMARK}(f_{vib})} \cdot 100$$

Equation (35)

ΔP% depends on c^*, m^*, k_s^* and obviously on f_{vib}. For example, in Fig. 6, the pattern of ΔP% as a function of m^* and k_s^*, for a fixed value of c^* and f_{vib} is reported. For reasons of clarity of representation, in Fig. 6 the surface portion characterized by negative values of ΔP% has been replaced with a flat surface of zero value. This means that only the operating region has been highlighted where the SMDE MTT technique is of practical use. In Fig. 6, the horizontal axes report the normalized quantities k_s^*/k_s and m^*/m, while the used fixed normalized values of c^* and f_{vib} are: c^*/c = -1.6 and f_{Vib}/f_{opt} = 0.8. This means that a vibration frequency that is less (80%) than the original resonance frequency f_{opt} of REVEH 1 was considered.

The maximum value ΔP_{MAX}% of ΔP% in Fig. 6 is about 47% and is obtained at k_s^*/k_s = -0.76 and m^*/m = -0.94. In fact, for every

value of c^*, a pair of values of k_s^* and m^* exists for which $\Delta P\%$ assumes its maximum value $\Delta P_{MAX}\%$. In the following, the values of k_s^* and m^* which, for a given value of c^*, lead to the maximum value of $\Delta P\%$ will be indicated respectively as $k_{s\_BEST}^*$ and m_{BEST}^*. In practice, since the identification of the best performances that can be obtained when the SMDE MTT technique is applied to REVEH 1 is of interest, the identification of the absolute maximum $\Delta P_{MAX\_TOT}\%$ of $\Delta P_{MAX}\%$ is of interest. Thus, a number of numerical simulations have been performed with different values of c^*. For each value of c^*, the pair of values $k_{s\_BEST}^*$ and m_{BEST}^* have been numerically identified by means of appropriate scans of each of the two parameters (k_s^* and m^*). In Fig. 7a, the curve $\Delta P_{MAX}\%$ vs. c^*/c is reported at $f_{vib}/f_{opt} = 0.8$. The value $c^*/c = c_{BEST}^*/c = -0.4$ (c_{BEST}^* indicates the value of c^* which, for a given frequency $f_{v\pm b}$, allows to obtain the maximum value of $\Delta P\%$) allows to obtain $\Delta P_{MAX\_TOT\%} = 79\%$ (as shown in Fig. 7a). The corresponding values of m_{BEST}^*/m and k_{sBEST}^*/k_s are: $m_{BEST}^*/m = -0.51$ (as shown in Fig. 7b) and $k_{s\_BEST}^*/k_s = -0.58$ (as shown in Fig. 7c). Figure 7d also shows the pattern of normalized frequency $f_{opt\_BEST}^*/f_{vib}$ as a function of c^*/c at $f_{Vib}/f_{opt} = 0.8$. The value of $f_{opt\_BEST}^*$ has been identified according to equation (16) by using, for each value of c^*, the corresponding values of $k_{s\_BEST}^*$ and m_{BEST}^*. In practice, Fig. 7d clearly indicates that, for each value of c^*, in order to obtain the best performance, it is necessary to set the $f_{opt\_BEST}^*$ resonance frequency of the system to a value higher than the vibration frequency $f_{v\pm b}$. For example, at $f_{Vib}/f_{opt} = 0.8$, in the optimal operating point of the SMDE REVEH 1 ($c_{BEST}^*/c = -0.4$, $k_{sBEST}^*/ks = -0.58$, $m_{BEST}^*/m = -0.51$, $\Delta P_{MAX-TOT}\% = 79\%$, see Figures 7a-d) it is $f_{opt-BEST}^*/f_{vib} = 1.18$ (Fig. 7d). This is a completely unexpected result, as one

could intuitively expect that $f^*_{opt\_BEST}$ should be chosen to be coincident with f_{Vib} -

Figure 8, on the other hand, shows the pattern of m^*/m and $k_s{}^*/k_s$ (c^*/c = $CBEST^*/C$ = -0.4 and f_{vib}/f_{opt} = 0.8).

The curves shown in figure 9a, which refer to the maximum of the case shown in Fig. 8 (c^*/c = $c_{BEST}{}^*/C$ = -0.4, f_{vib}/f_{opt} = 0.8, $k_{s\_BEST}{}^*/k_s$ =-0.58, $m_{BEST}{}^*/m$ = -0.51), clearly indicate that $\Delta P\%$ takes on its maximum value ($\Delta P_{MAX\_TOT\%}$ = 79%) at f/f_{vib} = 1 when $f^*_{opt\text{-}BEST}/f_{vib}$ = 1.18 and f_{opt}/f_{vib} = 1/0.8 = 1.25. In other words, the best performances are obtained with an emulated resonance frequency $f^*_{opt\_BEST}$ which is greater than f_{vib}, but smaller than the original mechanical resonance frequency f_{opt} of REVEH. Note that, at f = f_{Vib}, PLO_AD_SMDE is positive and therefore represents a power that is supplied to the load. In other words, the flow direction of PLO_AD_SMDE goes from the internal coil 14 of the SMDE REVEH 1 towards the battery. Moreover, at f = f_{vib}, PSMDE is negative. This means that the electronic power converter that regulates the current in the external coil (Fig. 5) absorbs (and does not inject) power from this coil. Thus, the direction of the power flow of PSMDE goes from the external coil 15 of the SMDE REVEH 1 towards the battery. In conclusion, under the considered operating conditions, the power is supplied to the battery by both coils.

For completeness, Fig. 9b shows the patterns (Fourier transform module) , depending on the frequency, the load voltage (V_{LOAD_SMDE}) of the internal coil 14 of the SMDE REVEH 1 and that (V) of the internal coil of the ORIGINAL REVEH 1, i.e. of the conventional harvester. The same figure also shows the pattern as a function of the voltage frequency (V_{ext}) to the output of the electronic power converter which regulates the current in the external coil 15 of SMDE REVEH 1.

Furthermore, Fig. 9c reports the patterns (Fourier transform module) as a function of the load current frequency (I_{SMDE}) of the internal coil 14 of the SMDE REVEH 1 and of the load current (I) of the internal coil of the ORIGINAL REVEH 1, i.e. of the conventional harvester. The same figure also shows the pattern as a function of the frequency of the current (I_{ext}) injected by the power electronics converter into the external coil 15 of the SMDE REVEH 1.

As for the second considered harvester (REVEH 2), this is a device with the following mechanical parameters: m = 0.83 kg, k_s = 296 kN/m, c = 1.882 N-s/m, θ_{int} = 552.25 N/A, R_{c_int} = 99.5 Ω, L_{c_int} = 4 H. Its mechanical resonance frequency is f_{opt} = 95.1 Hz. At a = 100 mg (peak acceleration value) and at its resonance frequency, REVEH 2 is able to supply its maximum load with a power P_{MAX} = 2.7 mW. In Fig. 10, the pattern of ΔP% is reported as a function of m^*/m e k_s^*/k_s at f_{vib}/f_{opt} = 0.7 and c^*/c = c_{BEST}^*/c = -0.2 (which is the optimal value of c^*/c for SMDE REVEH 2). The corresponding maximum value ΔP_{MAX_TOT}% in Fig. 10 is equal to 161% and is obtained with k_{sBEST}^*/k_s = -0.656 and m_{BEST}^*/m = -0.625. In Fig. 11a, all the average powers of interest are reported ($k_{sBE}s_T^*/k_s$ = -0.656, $m_{BE}s_T^*/m$= -0.625, c^*/c = c_{BEST}^*/c = -0.2, f_{vib}/f_{opt} = 0.7). It is possible to make similar considerations to those that have already been discussed with reference to Fig. 9a and which are not repeated here for conciseness. For completeness, Figures lib and 11c also report the frequency patterns (Fourier transform module) of the main voltages and currents.

The comparison of figures 9(c) and 11(c) shows that the order of magnitude of the currents circulating in the two coils is almost the same.

In conclusion, the method to optimize the conversion of vibrational kinetic energy generated by an external source,

into electrical energy, uses the SMDE MTT technique to be applied to a REVEH-type harvester. The aforementioned technique is based on the adoption of an external coil to be added to the standard architecture of a REVEH. The resulting REVEH (SMDE REVEH) is composed of two coils: an external coil 15 anchored to a fixed non-vibrating point and an internal coil 14 anchored to the REVEH casing 10. The current which circulates in the external coil 15 must be appropriately adjusted by means of a specific power electronics converter 17 (or electrical control circuit) so as to allow the emulation of the desired mass-spring-damper system. In this description the guidelines for the identification of operating conditions have also been proposed, leading to a positive net energy balance for the SMDE REVEH. Two different REVEHs were analysed numerically. The results of the numerical simulations have clearly shown that, in both cases, the proposed technique is efficient for vibration frequencies f_{vib} that are lower than the mechanical resonance frequency f_{opt} originating from the REVEH. In particular, in order to optimize the performance of the SMDE REVEH, the new mechanical resonance frequency $f^*_{opt\_BEST}$ must be set lower than the frequency f_{opt} but higher than the vibration frequency f_{vib}.

The proposed method is also applicable to other types of harvesters such as magnetostrictive or piezoelectric types. In the case of piezoelectric harvester applications, it is possible to place a magnetic element at the tip of the piezoelectric cantilever and use a fixed coil whose current, appropriately controlled, allows to apply to the magnet a force necessary to vary the resonance frequency of the harvester by emulating an appropriate mass-spring-damper system.

A person skilled in the art can perform several and further modifications and variants to the harvester and the method

described above, in order to satisfy further and contingent needs, all said modifications and variants being however included within the scope of protection of the present invention as defined by the appended claims.

CLAIMS

1. Resonant vibration energy harvester (1) for optimizing the conversion of vibrational kinetic energy generated by an external source into electrical energy, the harvester comprising :

a supporting housing (10) capable of vibrating in response to the external source; and

an electromagnetic generator (11) coupled to the housing (10) and having a resonance frequency, wherein the generator (11) comprises:

elastic means (12) placed within the housing (10) and fixed to a wall of said housing (10);

at least one magnetic element (13), having a mass (m) and coupled to the housing (10) by said elastic means (12), wherein said elastic means (12) create a relative motion between the magnetic element (13) and the housing (10) itself and wherein the magnetic element (13) is a permanent magnet and the resonance frequency of the electromagnetic generator (11) is the mechanical resonance frequency of the magnetic element (13) with respect to the housing (10); and

a first conductive winding (14) magnetically coupled to the magnetic element (13) and fixed to the housing (10) such that the vibrational kinetic energy generated by the external source determines a relative displacement (x) between the magnetic element (13) and the first winding (14) causing a potential difference to be generated at the ends of the first winding (14),

characterized by the fact that

the harvester (1) further comprises a second conductive winding (15) fixed to a non-vibrating support (16) and being stationary with respect to said support (16) and separated

from the housing (10), wherein the distance between the first winding (14) and the second winding (15) is such as to make a mutual magnetic coupling between said first and second winding (14, 15) negligible; and

control means (17) connected to the ends of the second winding (15) to introduce an electric current within the second winding (15) and regulate the intensity of said electric current so as to adapt the resonance frequency of the electromagnetic generator (11) to the vibration frequency associated to the vibrational kinetic energy generated by the external source.

2. Harvester (1) according to claim 1, wherein the elastic means (12) comprise a couple of coil springs each having one end fixed to the housing (10) and the other end fixed to the magnetic element (13).

3. Harvester (1) according to one of the preceding claims, further comprising an extraction electrical circuit and a storage circuit coupled to the ends of the first winding (14).

4. Harvester (1) according to one of the preceding claims, wherein the first and the second winding (14, 15) are positioned on the opposite sides with respect to the magnetic element (13).

5. Harvester (1) according to one of the preceding claims, wherein the control means (17) comprise a control electrical circuit for the generation of electrical current and the consequent emulation of a mass-spring-damper system.

6. Harvester (1) according to claim 5, wherein the control electrical circuit (17) is configured to determine an emulated resonance frequency with a value that is higher than the vibration frequency and lower than the resonance frequency of the electromagnetic generator (11).

7. Harvester (1) according to one of the preceding claims, wherein the dimensions of the first winding (14) are different from those of the second winding (15).

8. System comprising a resonant vibration energy harvester (1) according to one of the claims from 1 to 7 and an electronic device coupled to said harvester (1).

9. Method for optimizing the conversion of vibrational kinetic energy generated by an external source into electrical energy, wherein the method comprises:

providing a supporting housing (10) capable of vibrating in response to the external source; and

coupling an electromagnetic generator (11) having a resonance frequency to the housing (10), wherein the generator (11) comprises elastic means (12) placed within the housing (10) and fixed to a wall of said housing (10), at least one magnetic element (13) having a mass (m) and coupled to the housing (10) by said elastic means (12), wherein said elastic means (12) create a relative motion among the magnetic element (13) and the housing (10) itself and wherein the magnetic element (13) is a permanent magnet and the resonance frequency of the electromagnetic generator (11) is the mechanical resonance frequency of the magnetic element (13) with respect to the housing (10) and a first conductive winding (14), magnetically coupled to the magnetic element (13) and fixed to the housing (10) such that the vibrational kinetic energy generated by the external source determines a relative displacement (x) between the magnetic element (13) and the first winding (14) causing a potential difference to be generated at the ends of the first winding (14),

characterized by:

providing a second conductive winding (15) fixed to a non-vibrating support (16) and being stationary with respect to said support (16) and separated from the housing (10), wherein the distance between the first winding (14) and the second winding (15) is such as to make a mutual magnetic coupling between said first and second winding (14, 15) negligible; and

connecting control means (17) to the ends of the second winding (15), to inject an electric current within the second winding (15) and regulate the intensity of said electric current so as to adapt the resonance frequency of the electromagnetic generator (11) to the frequency or to the frequencies associated to the vibrational kinetic energy generated by the external source.

10. Method according to claim 9, further comprising emulating a mass-spring-damper system as a consequence of the introduction of electric current within the second winding (15) by connecting the control means (17) to the ends of the second winding (15).

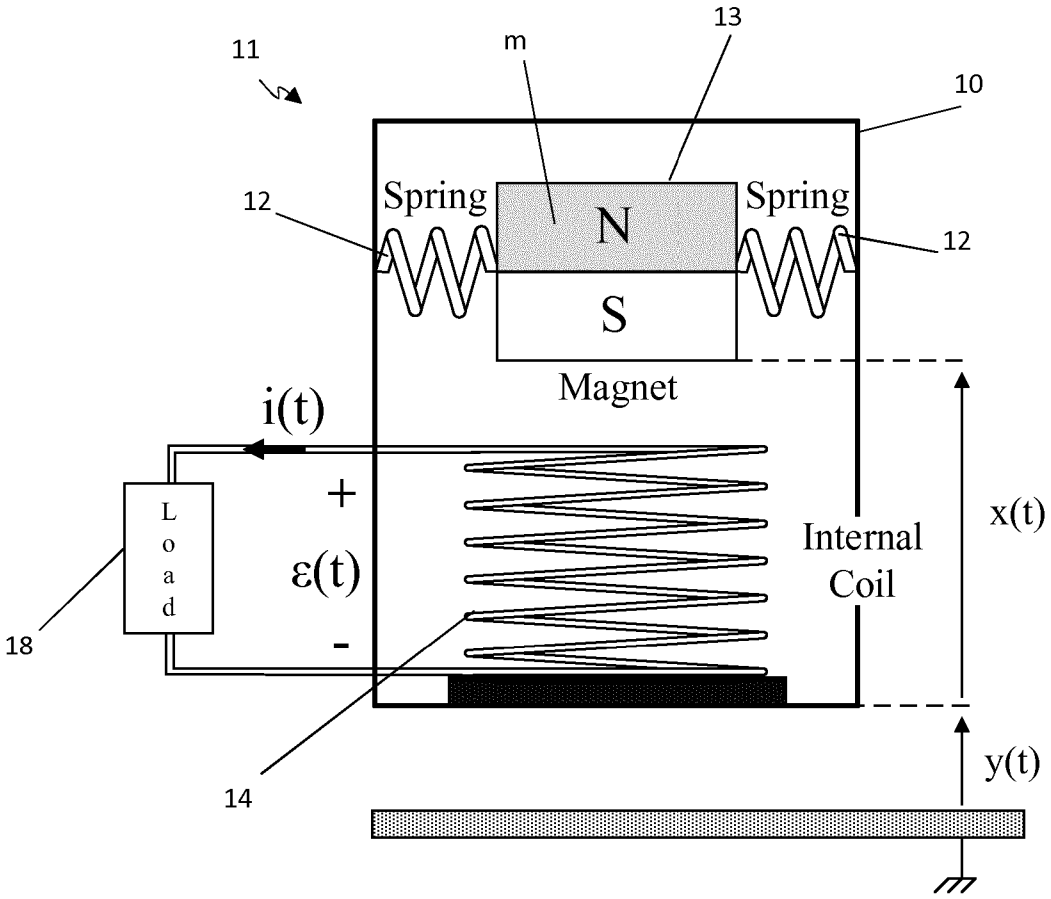
11
m
13
10
12
Spring
N
Spring
12
S
Magnet
i(t)
+
ε(t)
-
Load
18
Internal
Coil
x(t)
y(t)
14

Fig. 1

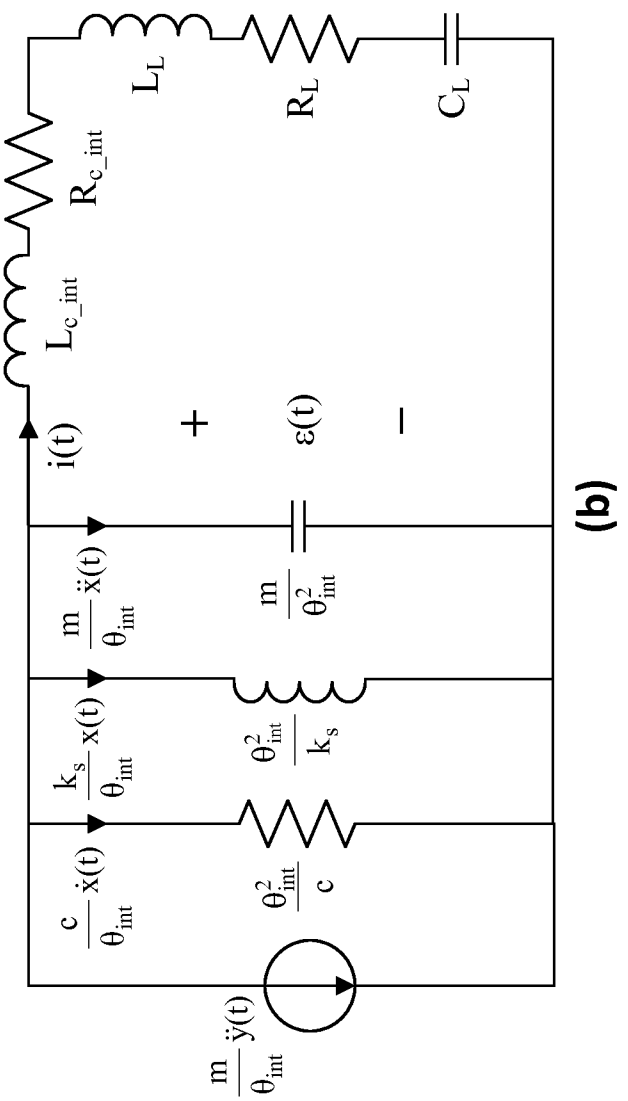
L_L
R_L
C_L
R_{c_int}
L_{c_int}
i(t)
+
ε(t)
−
$\frac{m}{\theta_{int}^2}$
$\frac{m}{\theta_{int}}\ddot{x}(t)$
$\frac{k_s}{\theta_{int}}x(t)$
$\frac{\theta_{int}^2}{k_s}$
$\frac{c}{\theta_{int}}\dot{x}(t)$
$\frac{\theta_{int}^2}{c}$
$\frac{m}{\theta_{int}}\ddot{y}(t)$
(b)

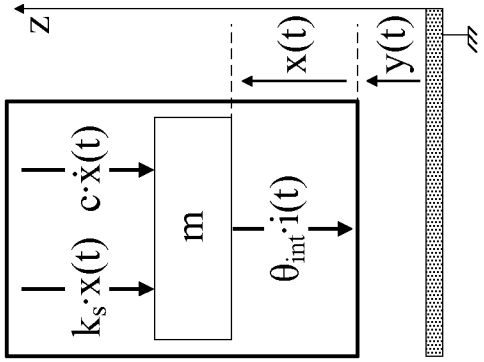
z
x(t)
y(t)
$k_s \cdot x(t)$
$c \cdot \dot{x}(t)$
m
$\theta_{int} \cdot i(t)$
(a)

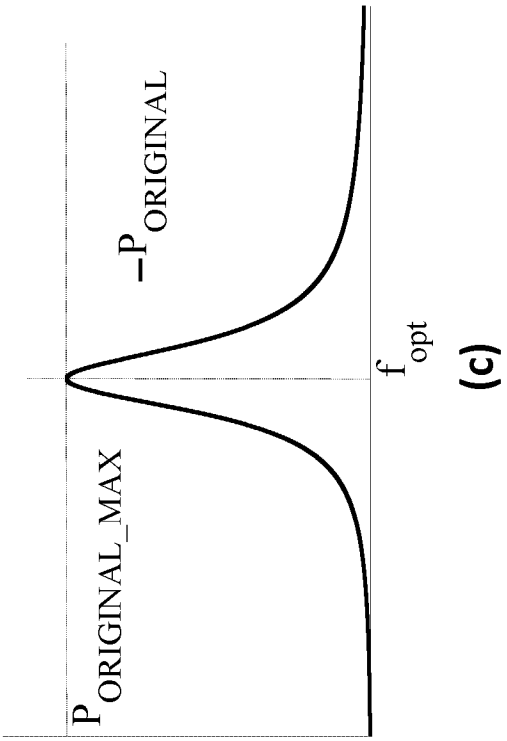
$P_{ORIGINAL\_MAX}$
$-P_{ORIGINAL}$
f_{opt}
(c)

Fig. 2

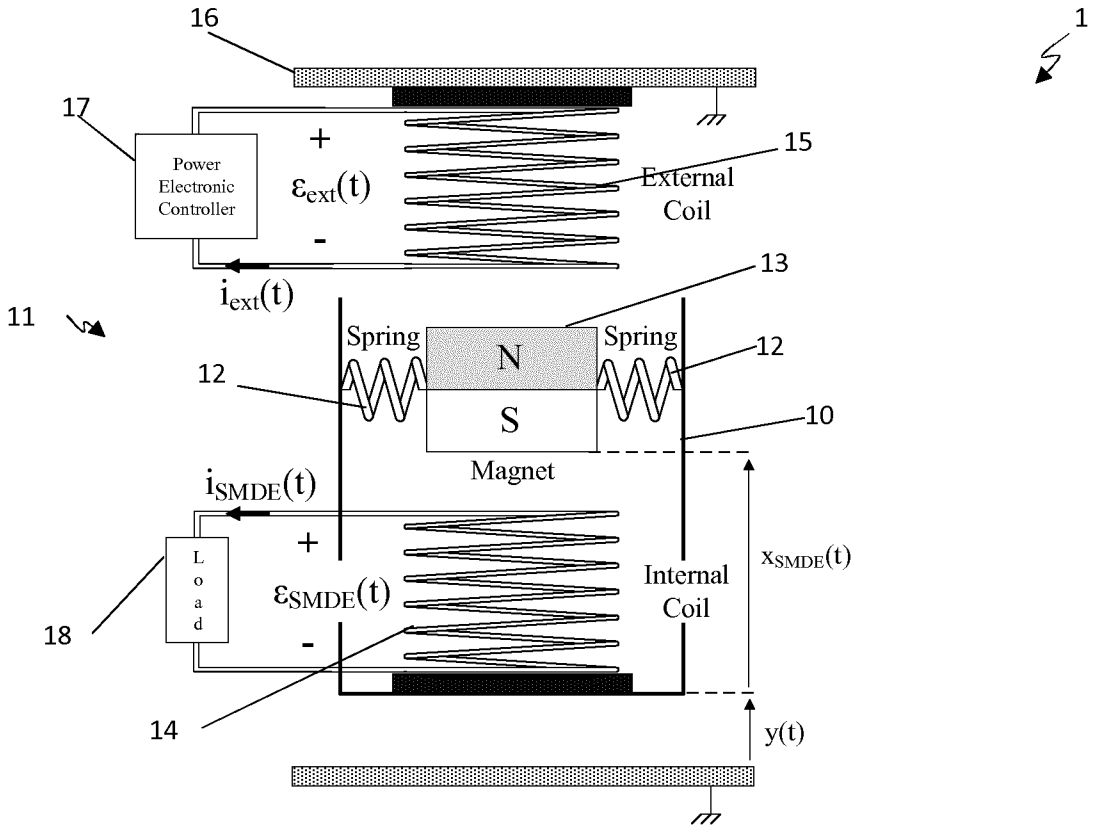
16
1
17
Power Electronic Controller
+
$\varepsilon_{ext}(t)$
-
15
External Coil
$i_{ext}(t)$
13
11
Spring
N
Spring
12
12
S
10
Magnet
$i_{SMDE}(t)$
+
$\varepsilon_{SMDE}(t)$
-
Load
18
Internal Coil
$x_{SMDE}(t)$
14
y(t)

Fig. 3

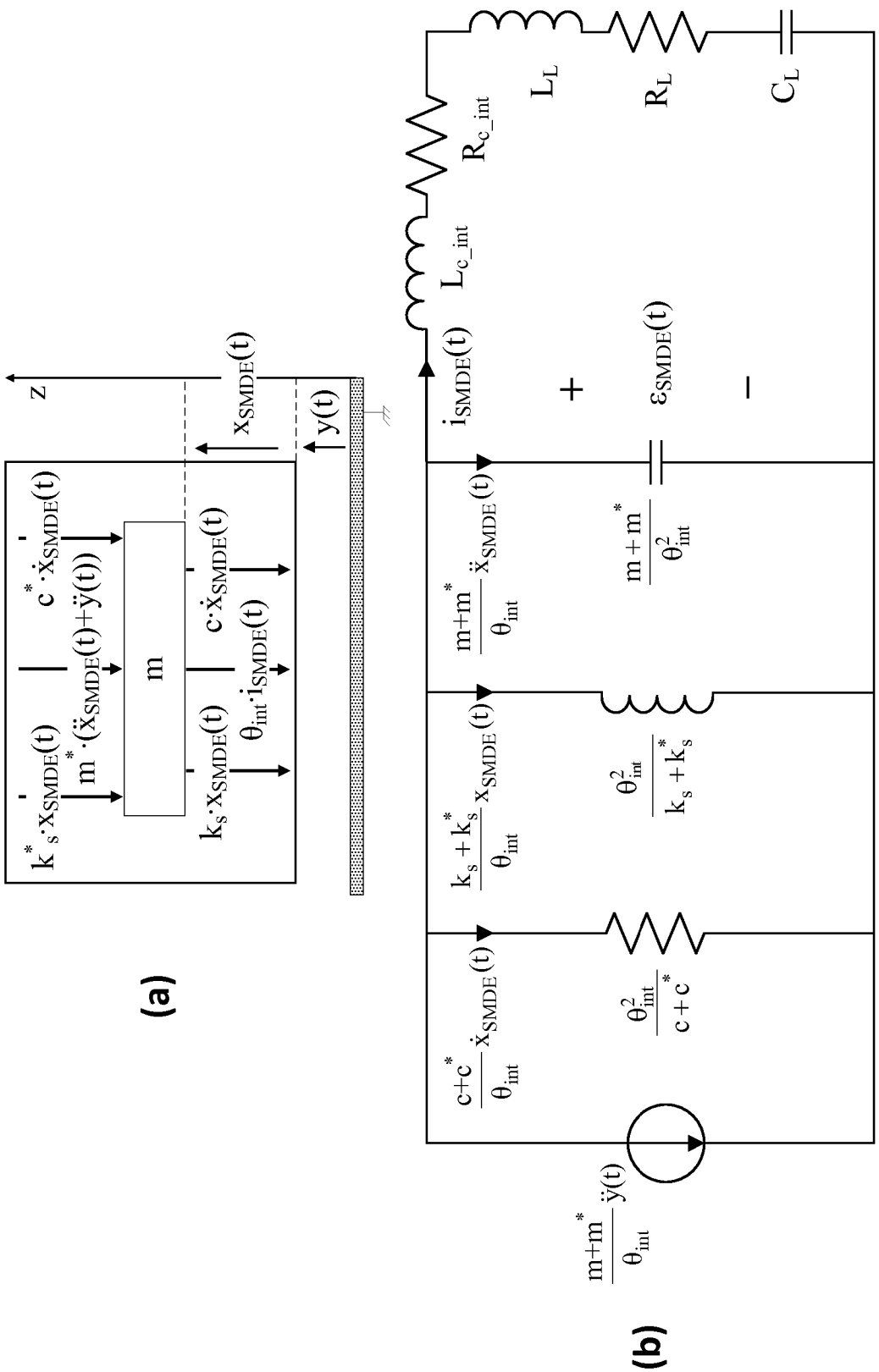
(a)
z
$x_{SMDE}(t)$
y(t)
$k^*_s \cdot x_{SMDE}(t)$
$c^* \cdot \dot{x}_{SMDE}(t)$
$m^* \cdot (\ddot{x}_{SMDE}(t)+\ddot{y}(t))$
m
$k_s \cdot x_{SMDE}(t)$
$c \cdot \dot{x}_{SMDE}(t)$
$\theta_{int} \cdot i_{SMDE}(t)$
(b)
R_{c_int}
L_{c_int}
$i_{SMDE}(t)$
L_L
R_L
C_L
+
$\varepsilon_{SMDE}(t)$
–
$\frac{m+m^*}{\theta_{int}^2}$
$\frac{m+m^*}{\theta_{int}} \ddot{x}_{SMDE}(t)$
$\frac{\theta_{int}^2}{k_s+k_s^*}$
$\frac{k_s+k_s^*}{\theta_{int}} x_{SMDE}(t)$
$\frac{\theta_{int}^2}{c+c^*}$
$\frac{c+c^*}{\theta_{int}} \dot{x}_{SMDE}(t)$
$\frac{m+m^*}{\theta_{int}} \ddot{y}(t)$

Fig. 4

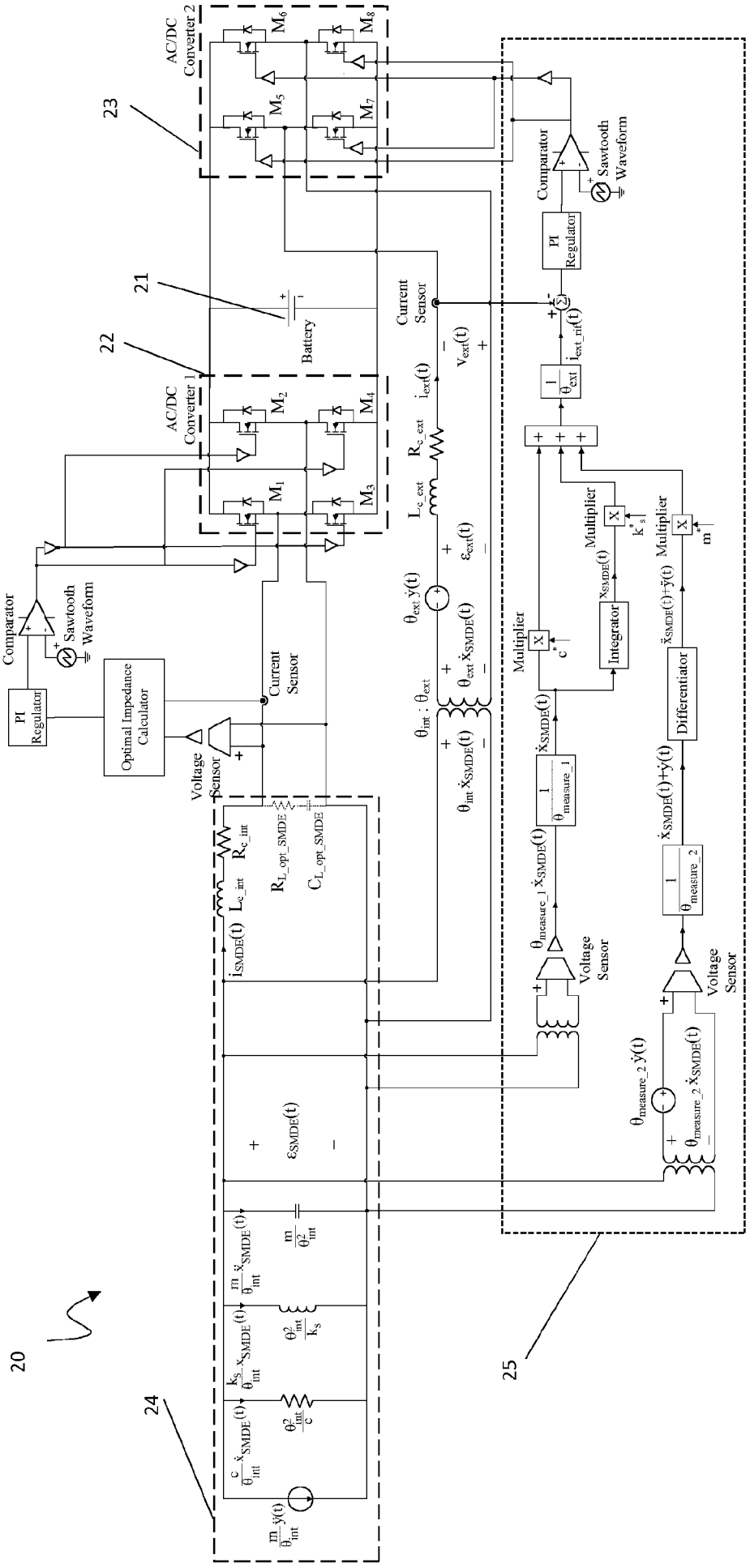
20
21
22
23
24
25
AC/DC Converter 1
AC/DC Converter 2
Battery
Current Sensor
Voltage Sensor
Comparator
Sawtooth Waveform
PI Regulator
Optimal Impedance Calculator
Multiplier
Integrator
Differentiator

Fig. 5

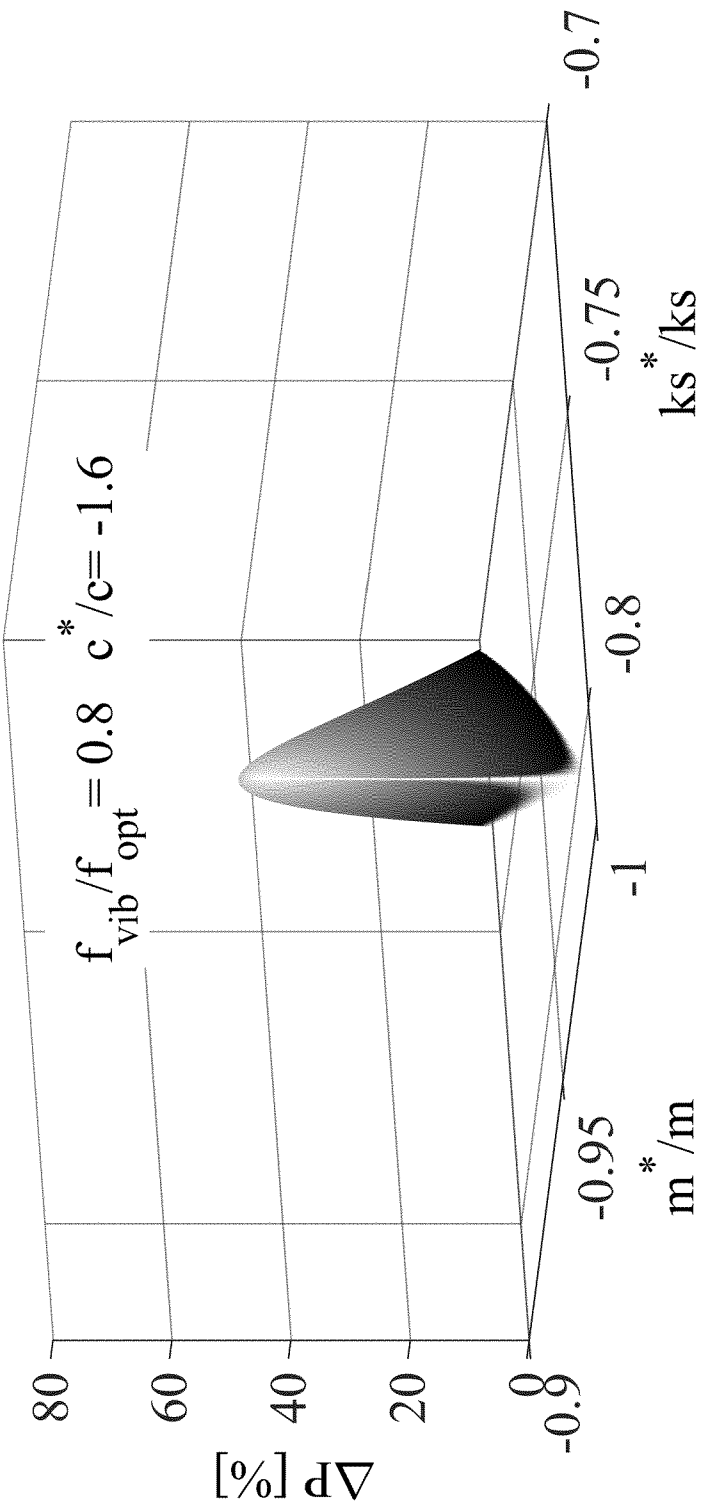

Fig. 6

(a)

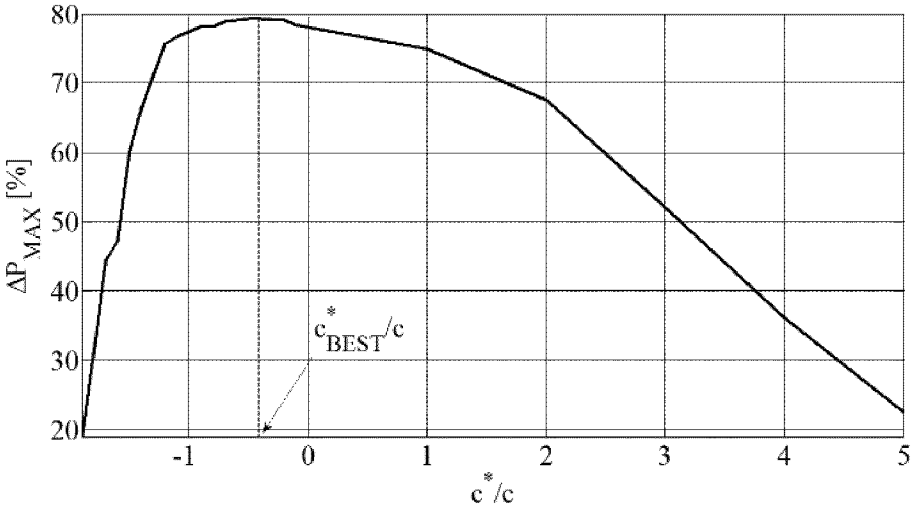
80
70
60
50
40
30
20
ΔP_MAX [%]
c*_BEST/c
-1
0
1
2
3
4
5
c*/c

(b)

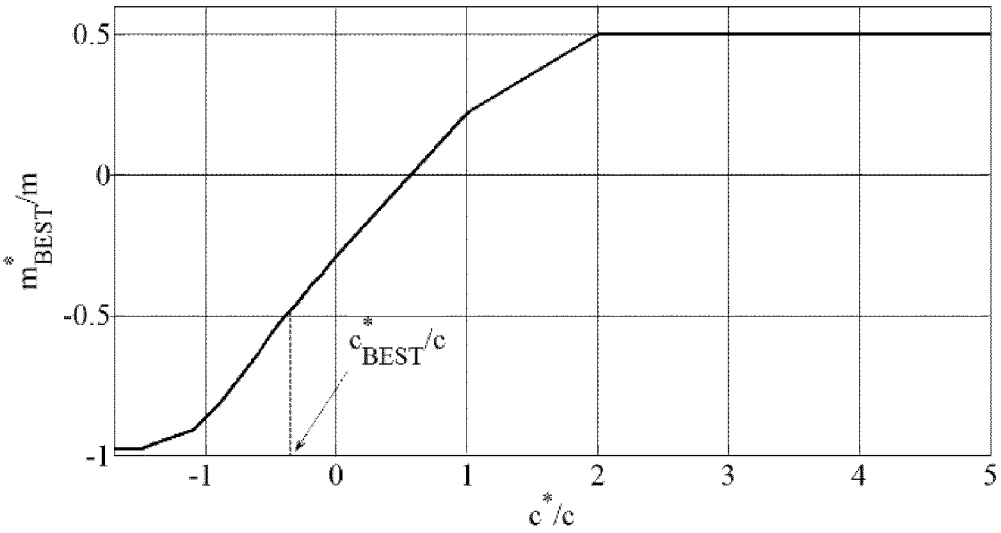
0.5
0
-0.5
-1
m*_BEST/m
c*_BEST/c
-1
0
1
2
3
4
5
c*/c

Fig. 7 (1/2)

(c)

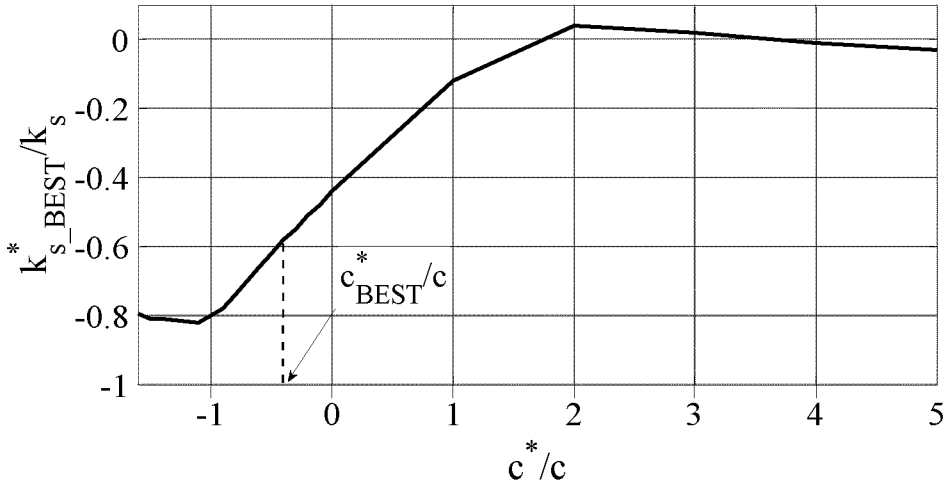
0
-0.2
-0.4
-0.6
-0.8
-1
$k^*_{s\_BEST}/k_s$
c^*_{BEST}/c
-1
0
1
2
3
4
5
c^*/c

(d)

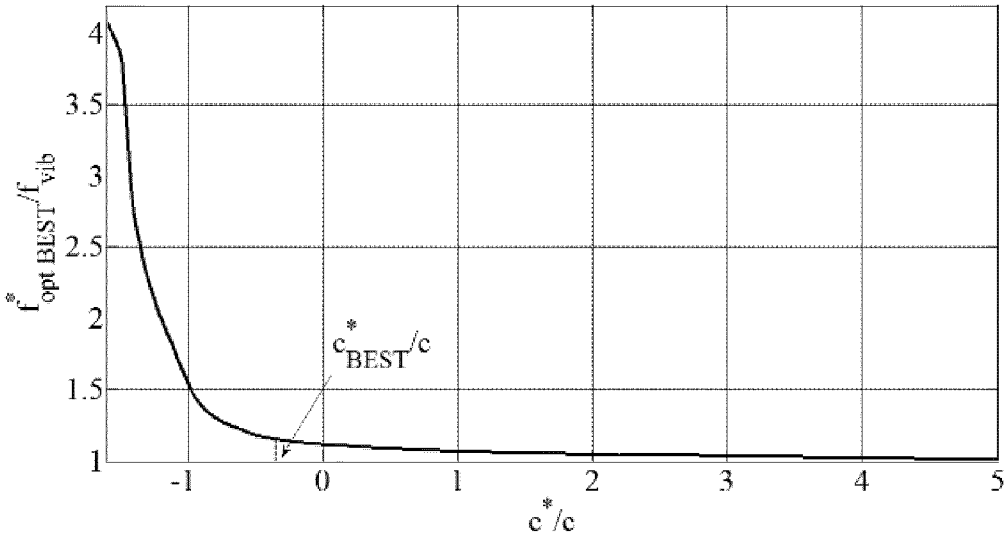
4
3.5
3
2.5
2
1.5
1
$f^*_{opt\ BEST}/f_{vib}$
c^*_{BEST}/c
-1
0
1
2
3
4
5
c^*/c

Fig. 7 (2/2)

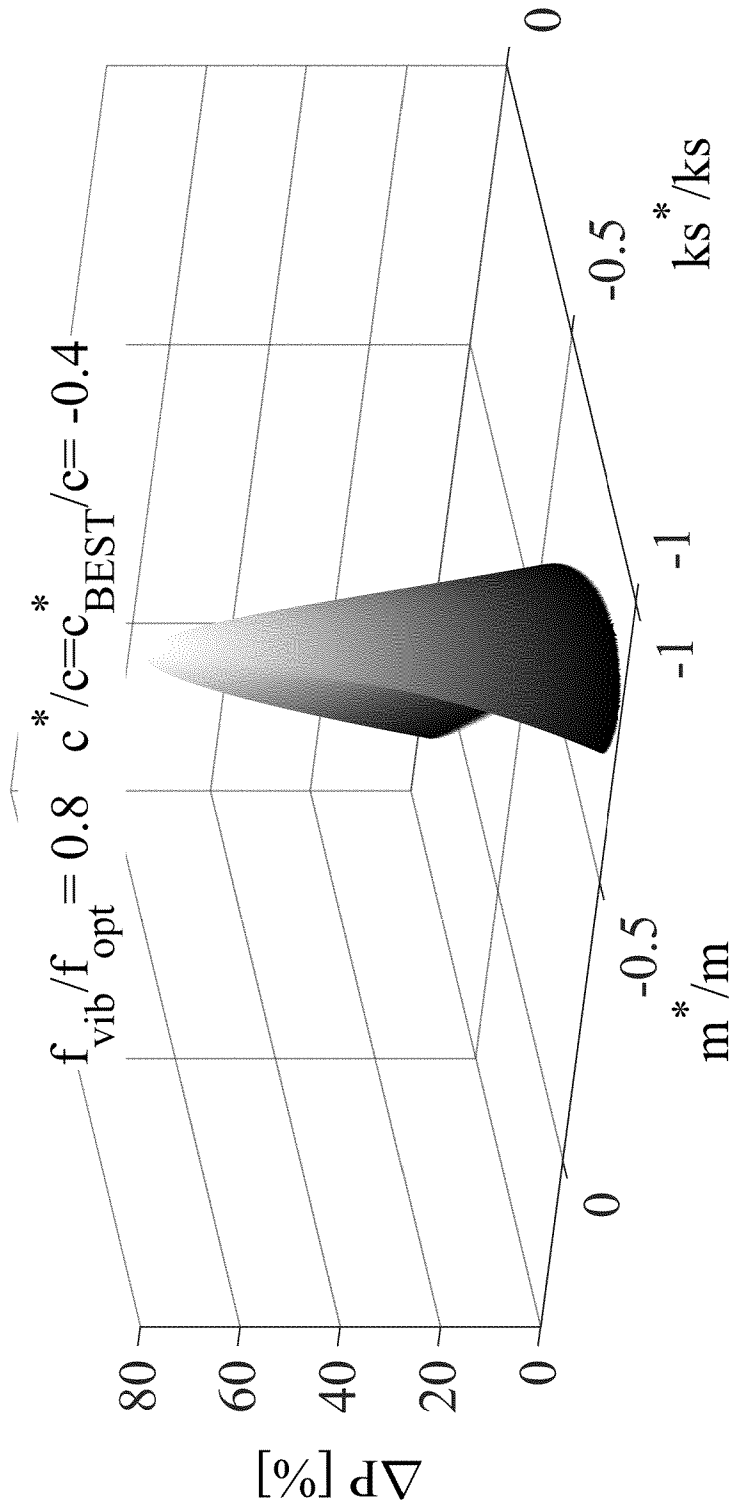

Fig. 8

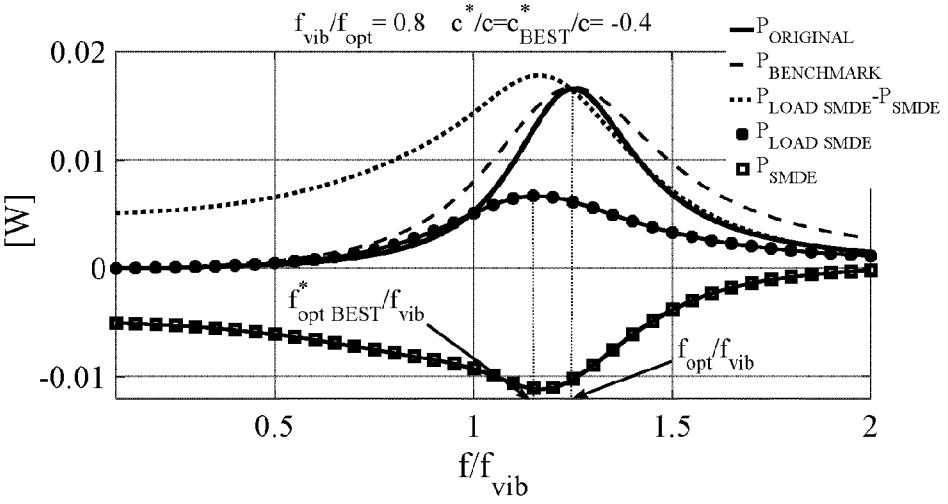
f_{vib}/f_{opt} = 0.8 $c^*/c=c^*_{BEST}/c$= -0.4
$P_{ORIGINAL}$
$P_{BENCHMARK}$
$P_{LOAD\ SMDE}$-P_{SMDE}
$P_{LOAD\ SMDE}$
P_{SMDE}
[W]
0.02
0.01
0
-0.01
$f^*_{opt\ BEST}/f_{vib}$
f_{opt}/f_{vib}
0.5
1
1.5
2
f/f_{vib}

(a)

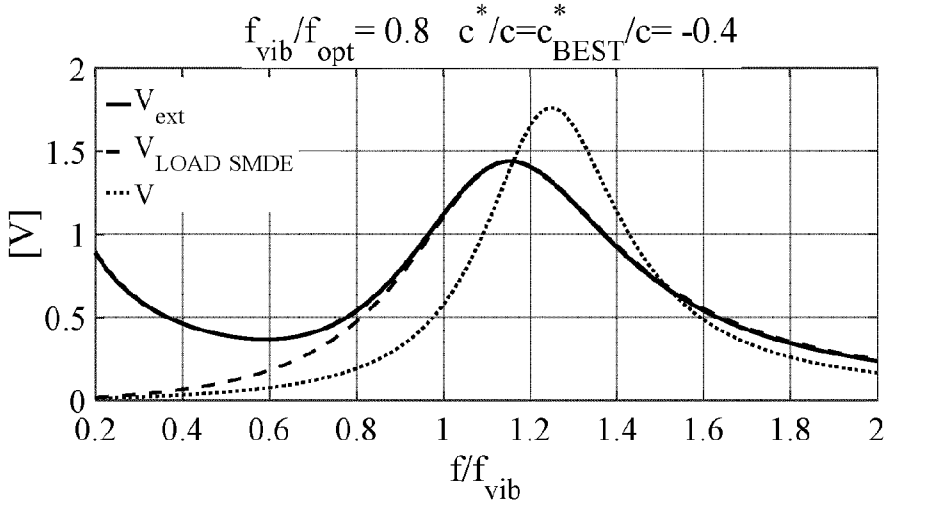
f_{vib}/f_{opt} = 0.8 $c^*/c=c^*_{BEST}/c$= -0.4
V_{ext}
$V_{LOAD\ SMDE}$
V
[V]
2
1.5
1
0.5
0
0.2
0.4
0.6
0.8
1
1.2
1.4
1.6
1.8
2
f/f_{vib}

(b)

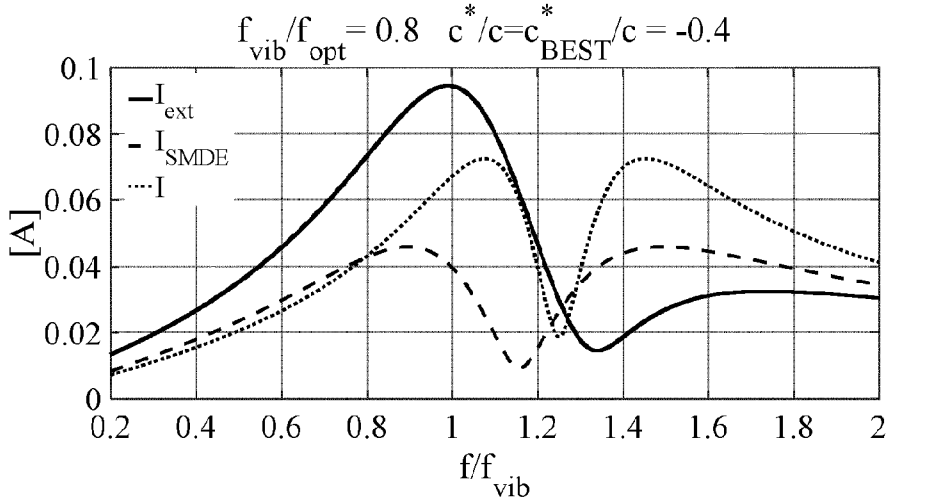
f_{vib}/f_{opt} = 0.8 $c^*/c=c^*_{BEST}/c$ = -0.4
I_{ext}
I_{SMDE}
I
[A]
0.1
0.08
0.06
0.04
0.02
0
0.2
0.4
0.6
0.8
1
1.2
1.4
1.6
1.8
2
f/f_{vib}

(c)

Fig. 9

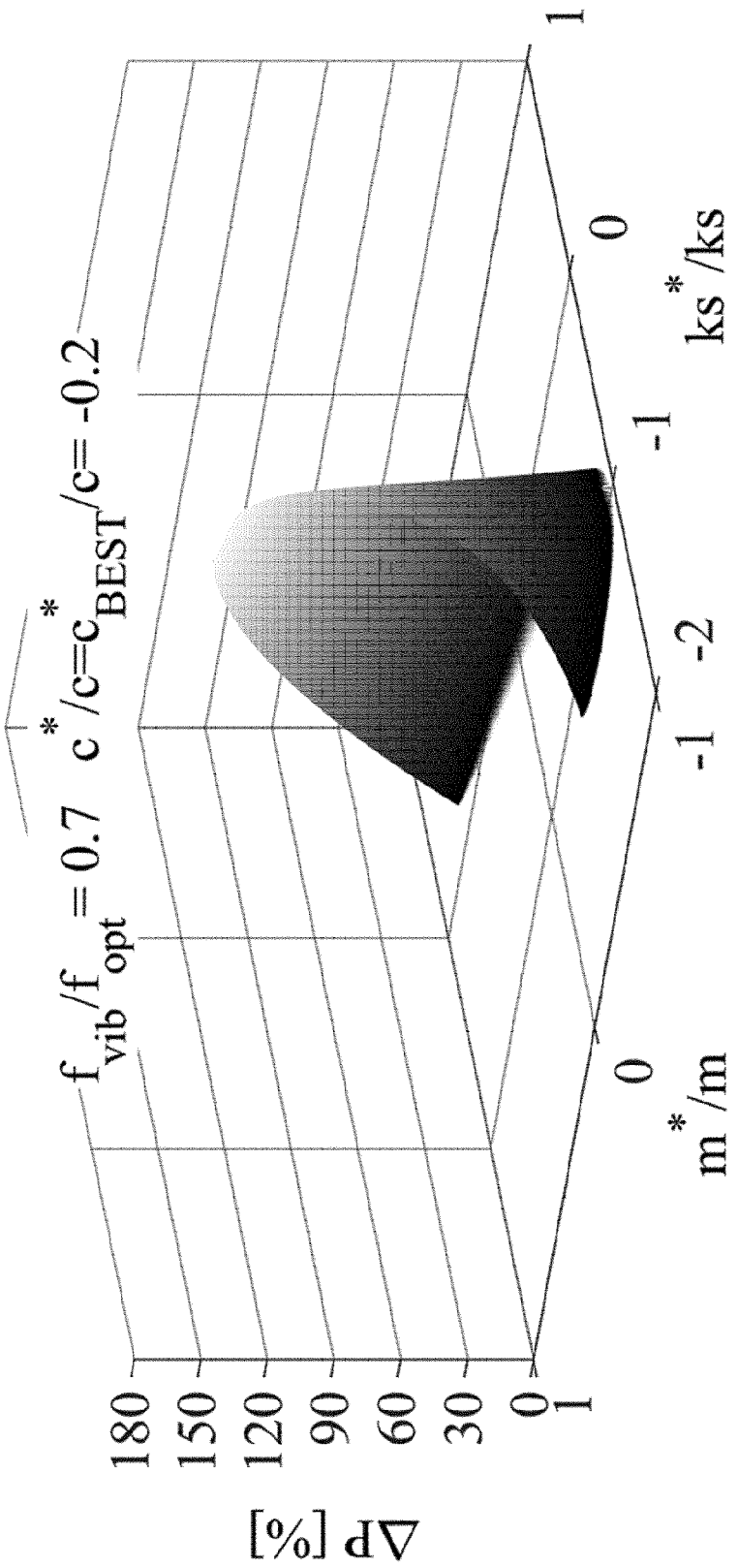
ΔP [%]
180
150
120
90
60
30
0
1
0
-1
-2
-1
0
1
m*/m
ks*/ks
f_vib/f_opt = 0.7 c*/c=c*_BEST/c= -0.2

Fig. 10

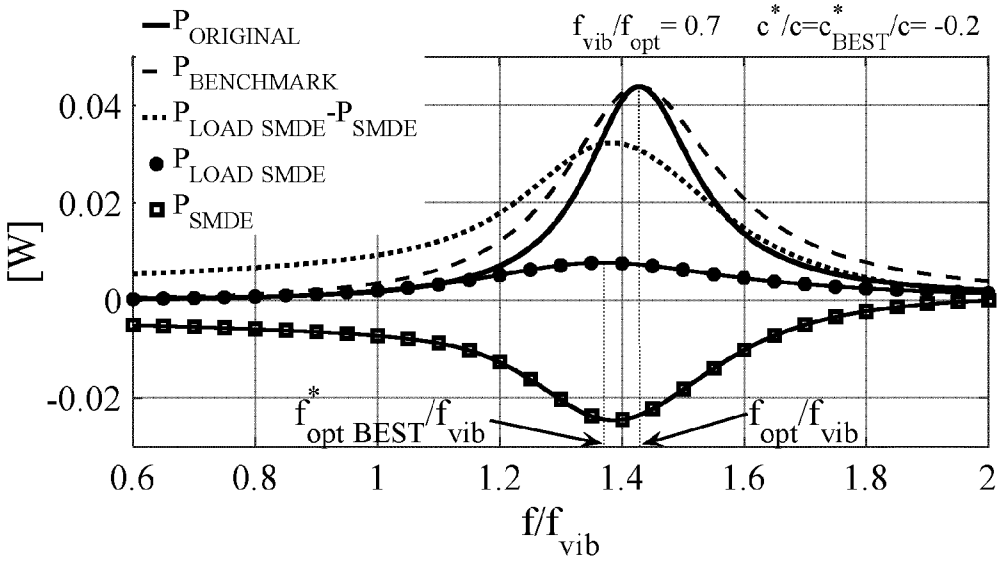
P ORIGINAL
P BENCHMARK
P LOAD SMDE -P SMDE
P LOAD SMDE
P SMDE
f vib/f opt = 0.7 c*/c=c* BEST/c= -0.2
0.04
0.02
0
-0.02
[W]
f* opt BEST/f vib
f opt/f vib
0.6 0.8 1 1.2 1.4 1.6 1.8 2
f/f vib

(a)

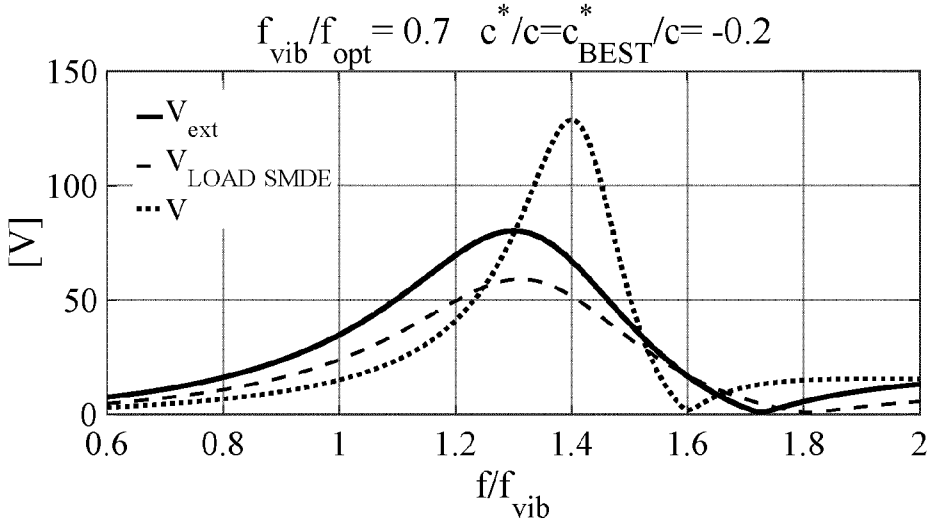
f vib/f opt = 0.7 c*/c=c* BEST/c= -0.2
V ext
V LOAD SMDE
V
150
100
50
0
[V]
0.6 0.8 1 1.2 1.4 1.6 1.8 2
f/f vib

(b)

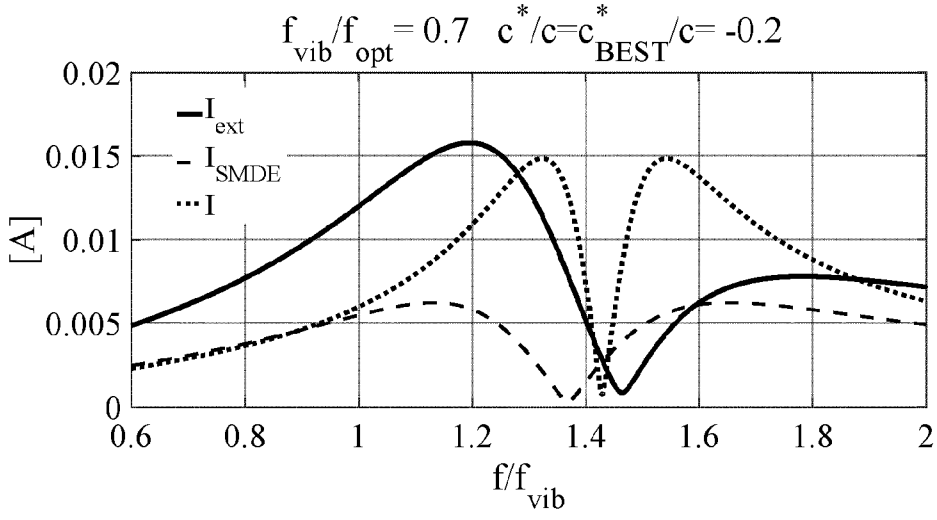
f vib/f opt = 0.7 c*/c=c* BEST/c= -0.2
I ext
I SMDE
I
0.02
0.015
0.01
0.005
0
[A]
0.6 0.8 1 1.2 1.4 1.6 1.8 2
f/f vib

(c)

Fig. 11

INTERNATIONAL SEARCH REPORT

International application No
PCT/EP2019/056601

A. CLASSIFICATION OF SUBJECT MATTER
INV. H02K33/02 H02K7/18 H02K35/02 H02N2/18
ADD.

According to International Patent Classification (IPC) or to both national classification and IPC

B. FIELDS SEARCHED

Minimum documentation searched (classification system followed by classification symbols)
H02K H02N

Documentation searched other than minimum documentation to the extent that such documents are included in the fields searched

Electronic data base consulted during the international search (name of data base and, where practicable, search terms used)
EPO-Internal , WPI Data

C. DOCUMENTS CONSIDERED TO BE RELEVANT

Category*	Citation of document, with indication, where appropriate, of the relevant passages	Relevant to claim No.
A	US 2010/194117 A1 (PABON JAHIR A [US] ET AL) 5 August 2010 (2010-08-05) abstract; figures 2,5,6,9, 10 paragraphs [0001], [0006] - [0010], [0027], [0028], [0035]	1-10
A	DE 10 2009 021556 A1 (EADS DEUTSCHLAND GMBH [DE]) 16 December 2010 (2010-12-16) abstract; figures 1-5 paragraphs [0025], [0044], [0057]	1-10
A	WO 2017/172012 A1 (INTEL CORP [US]) 5 October 2017 (2017-10-05) paragraphs [0024] - [0026], [0049]; figures 1-7	1-10

☐ Further documents are listed in the continuation of Box C.

☒ See patent family annex.

* Special categories of cited documents :

"A" document defining the general state of the art which is not considered to be of particular relevance

"E" earlier application or patent but published on or after the international filing date

"L" document which may throw doubts on priority claim(s) orwhich is cited to establish the publication date of another citation or other special reason (as specified)

"O" document referring to an oral disclosure, use, exhibition or other means

"P" document published prior to the international filing date but later than the priority date claimed

"T" later document published after the international filing date or priority date and not in conflict with the application but cited to understand the principle or theory underlying the invention

"X" document of particular relevance; the claimed invention cannot be considered novel or cannot be considered to involve an inventive step when the document is taken alone

"Y" document of particular relevance; the claimed invention cannot be considered to involve an inventive step when the document is combined with one or more other such documents, such combination being obvious to a person skilled in the art

"&" document member of the same patent family

Date of the actual completion of the international search	Date of mailing of the international search report
30 April 2019	08/05/2019

Name and mailing address of the ISA/	Authorized officer
European Patent Office, P.B. 5818 Patentlaan 2 NL - 2280 HV Rijswijk Tel. (+31-70) 340-2040, Fax: (+31-70) 340-3016	Ganchev, Martin

1

INTERNATIONAL SEARCH REPORT

Information on patent family members

International application No
PCT/EP2019/056601

Patent document cited in search report	Publication date	Patent family member(s)	Publication date
US 2010194117 A1	05-08-2010	EP 2394355 A2	14-12-2011
		US 2010194117 A1	05-08-2010
		WO 2010091156 A2	12-08-2010
DE 102009021556 A1	16-12-2010	NONE	
WO 2017172012 A1	05-10-2017	US 2017288443 A1	05-10-2017
		WO 2017172012 A1	05-10-2017